Deep–Sea Research II xxx (xxxx) xxx

Contents lists available at ScienceDirect

Deep-Sea Research Part II

journal homepage: http://www.elsevier.com/locate/dsr2

Ecology of mesozooplankton across four North Atlantic basins

Espen Strand *, Thor Klevjer, Tor Knutsen, Webjørn Melle

Institute of Marine Research, Postboks 1870 Nordnes, 5817, Bergen, Norway

ARTICLE INFO

Keywords:
North Atlantic
Mesozooplankton community
Calanus
Zooplankton biomass
Vertical distribution
Stage composition

ABSTRACT

A comparative study of the mesozooplankton in four North Atlantic basins is presented. During a trans-Atlantic expedition with R/V G.O. Sars in May and June 2013, the Norwegian Sea, Iceland Sea, Irminger Sea and Labrador Sea was surveyed twice on a round trip from Bergen, Norway to Nuuk, Greenland. Mesozooplankton samples of biomass, species composition and vertical distribution were obtained with WP2 and MOCNESS plankton nets, in addition to *in situ* data obtained from a Video Plankton Recorder (VPR) and Optical Plankton Counter (OPC) mounted on a submersible towed vehicle. Size-fractionated biomass samples showed that the Norwegian Sea had the highest biomass of small mesozooplankton (180–1000 μm), while Irminger and Iceland Seas had the highest biomass of the medium (1000–2000 μm) and largest (>2000 μm) size fractions, respectively. The Icelandic Sea large fraction biomass was dominated by Amphipods, Chaetognaths, Krill and *Calanus hyperboreus*. The Labrador Sea had the lowest total mesozooplankton biomass. A total of 9 different species/groups were found to comprise the 5 most numerically dominant species/groups across all basins, with *Oithona* spp. being the most common genus in all basins. *C. finmarchicus* was, as expected, found to be the most numerically common species of the *Calanus* complex in all basins, but the stage composition varied markedly between basins with young copepodite stages dominating only in the Labrador and central Norwegian Seas. In terms of both abundance and biomass, the Iceland Sea had a higher fraction of dominating mesozooplankton distributed below 200 m. The highest average particle density per 25 m interval was registered in the Norwegian Sea during daytime between 25-50 m (OPC data). In the Labrador and Irminger Seas, total estimated particle densities in the upper 50 m were lower and the particle densities peaked at intermediate sizes (1–3 mm). In all basins there were differences in the particle densities estimated between day and night. Based on VPR data, the Irminger and Iceland Seas had the highest density of copepods registered in the upper 200 m, whereas in the Labrador Sea, the highest average copepod densities were registered at depth. Densities of gelatinous organisms were at least an order of magnitude higher in the Labrador and Irminger Seas than in the Iceland Sea.

1. Introduction

Mesozooplankton play a vital role in marine ecosystems as the main trophic link between primary producers and carnivorous predators. At high latitudes, due to the strong seasonality in solar influx and primary production, many species of mesozooplankton have adapted to the seasonality in food availability (Falk-Petersen et al., 2009). The northern North Atlantic Ocean basins span a latitudinal gradient from around 50 to 75 °N which affects the seasonality significantly. Therefore, the North Atlantic cannot be considered as one ecosystem where key mesozooplankton can successfully utilise a single set of fixed life history strategies in relation to the seasonality (Head et al., 2013; Melle et al., 2014). Large variations in the ocean circulation patterns across the North Atlantic (Reverdin et al., 2003; Blindheim, 2004; Holliday et al., 2006) is also an important factor for the observed regional differences in mesozooplankton community and life strategies (e.g. Sundby, 2000). During the Euro-BASIN cruise in 2013, four north Atlantic Ocean basins – the Norwegian Sea (Nor), Iceland Sea (Ice), Irminger Sea (Irm) and Labrador Sea (Lab), were surveyed and the objectives were to increase the understanding of the differences and similarities in mesozooplankton community structure, behaviour and population dynamics. In addition, knowledge about the mesozooplankton community is essential to tie the physics and ecology of theses basins together, ranging from hydrography (Drinkwater et al., this issue), phytoplankton (Naustvoll et al., this issue), micronekton (Klevjer et al., this issue a, b) and herring (Melle et al., this issue).

* Corresponding author.
E-mail address: espen.strand@hi.no (E. Strand).

https://doi.org/10.1016/j.dsr2.2020.104844
Received 31 January 2020; Received in revised form 14 July 2020; Accepted 26 July 2020
Available online 31 July 2020
0967-0645/© 2020 The Authors. Published by Elsevier Ltd. This is an open access article under the CC BY license (http://creativecommons.org/licenses/by/4.0/).

1.1. North Atlantic Ocean circulation and basin connectivity

All four seas covered during the cruise contains one or more deep basins (Melle et al., 2014), over which local gyres are believed to aid in the local retention and the closing of life-cycles of plankton populations. According to literature, *Calanus finmarchicus* has two main overwintering areas, the western one in the Labrador/Irminger Seas and the eastern in the southern Norwegian Sea (Conover, 1988; Planque et al., 1997; Heath et al., 2000, 2008; Head et al., 2003; Melle et al., 2004; Broms et al., 2009). The main overwintering areas are situated in the local gyres, and parts of the overwintering generation from these gyres seed the populations of the surrounding shelves and shallow seas (Sundby, 2000; Melle et al., 2014). The North Atlantic Current (NAC), crosses the Atlantic Ocean in a north-eastward direction between approximately 50 to 60 °N, bringing warm, saline water masses northwards. South of Iceland and west of the UK, the NAC splits into the Norwegian Atlantic Current heading into the Norwegian Sea, while the other branch flows into the Irminger Sea in a north-westward direction (Irminger Current, IC). The Norwegian Atlantic current flows northwards along the Norwegian coast bounded by the Norwegian Coastal Current (NCC, Sætre, 2007) to the east and the polar front between the Norwegian and Iceland Seas to the west (Blindheim, 2004). Flowing southward along the east coast of Greenland, is the East Greenland Current (EGC), bringing cold Arctic water masses southwards. North of Iceland, the EGC branches off into the Iceland Sea or continues south-west wards through the Denmark Strait into the Irminger Sea. The Iceland Sea branch moves counter-clockwise where it meets the Norwegian Sea Current and becomes part of the Norwegian Sea gyre. The cyclonic Norwegian Sea gyre of the Norwegian Sea basin is an important retention area that has been shown to be a major production area for *C. finmarchicus*, which is likely the most important mesozooplankton species in the North Atlantic (Aksnes and Blindheim, 1996; Heath et al., 2000, 2008; Melle et al., 2004, 2014; Head et al., 2013). In the north-eastern Irminger Sea, the EGC meets the NAC branch which turns counter-clockwise and they follow the Greenland coast south-westwards with the EGC closest to the Greenland coast. The two currents continue next to each other around the southern tip of Greenland before moving northwards into the Labrador Sea basin where they slowly turn counter-clockwise and flow along Canadian coast southwards. This circulation pattern is considered the northern boundary of the Subpolar gyre, also considered to be a major retention area for mesozooplankton and thus important for mesozooplankton production (Planque et al., 1997; Heath et al., 2008). Due to the predominantly northward flow of warm Atlantic water on the east side of the north Atlantic (Norwegian Atlantic Current) and the southwards moving cold Arctic water in the central (EGC) and west (Labrador current) North Atlantic, the temperature isolines across the North Atlantic does not follow a latitudinal gradient as should be expected if solar influx where the determining cause. Instead, habitats within certain temperature regimes are found at high latitudes in the east while further south in the west (Planque et al., 1997; Sundby, 2000). Species with specific temperature niches can therefore be expected to be found at higher latitudes in the northeast Atlantic than in the northwest Atlantic. Thus, the same species might experience different levels of seasonality, particularly in solar influx, which may further affect life history strategies such as onset or termination of dormancy as well as timing of reproduction (Melle et al., 2014).

1.2. Mesozooplankton community

Previous studies have found the overall mesozooplankton biomass in the different regions to be dominated by a few important species. In the Labrador Sea, the 3 species of *Calanus* usually make up >70% of copepod biomass (Head et al., 2003), with *C. finmarchicus* usually alone making up more than 60% of total biomass and 80% of the total number of large copepods in spring and summer. In the Irminger Sea, *C. glacialis* and *C. hyperboreus* are usually found to be of lesser importance, but 5 copepod taxa (*C. finmarchicus, Paraeuchaeta norvegica, C. hyperboreus, Oithona* spp. and *Oncaea* spp.) usually constitute more than 95% of total copepod biomass (Gislason, 2003). In the Iceland Sea, the mesozooplanktom community have been found to differ depending on the origin of the dominating water mass (Gislason and Silva, 2012). In Atlantic water masses, *C. finmarchicus* and *Pseudocalanus* spp. are the most abundant species, while *C. hyperboreus* and *C. glacialis* dominate in water masses of Arctic origin. A third more southerly and coastally influenced mesozooplankton community in the Iceland Sea, dominated by *Temora spp*. and *Acartia* spp. (Gislason and Silva, 2012), was not sampled during this Euro-BASIN cruise. The Norwegian Sea basin is mainly influenced by Atlantic water masses where *C. finmarchicus*, *Oithona* spp. and *Pseudocalanus* spp. are the numerically dominant mesozooplankton species (Wiborg, 1955; Tande et al., 2000; Strand et al., 2020). However, in the western part of the Norwegian Sea towards the Iceland Sea, water masses with an Arctic origin becomes more prominent, and with it a mesozooplankton community more dominated by Arctic species like *C. hyperboreus. C. finmarchicus*, however, remains an important part of that community as well (Broms et al., 2009; Bagøien et al., 2012). Even though significant variations in the mesozooplankton community is evident throughout the four basins, *C. finmarchicus* is generally assumed to be the dominant mesozooplankton species in high latitude North Atlantic water masses in terms of biomass and annual production (Planque et al., 1997; Planque and Batten, 2000; Head et al., 2013; Melle et al., 2014).

The wide extent and scope of the 2013 Euro-BASIN cruise, together with the use of both classic plankton nets and advanced optical sampling, will hopefully enable us to shed new light and insight on the mesozooplankton composition, biomass, phenology and vertical distribution, not previously attempted on a basin wide scale. This paper will thus present a comparative analysis of the ecology of the mesozooplankton community across four northern North Atlantic Ocean basins.

2. Material and methods

The data used in this investigation were gathered onboard the research vessel G.O. Sars on a round trip from Bergen, Norway to Nuuk, Greenland during the period 1 May - 14 June 2013 (Fig. 1). Both traditional nets and modern optic technology were used during the two surveys of the four ocean basins – The Norwegian, Iceland, Irminger and Labrador Seas. The results obtained by the plankton nets, WP2 (Fraser, 1966) and MOCNESS (Wiebe et al., 1985), as well as data from two optical instruments, the OPC (Herman, 1992) and VPR (Davis et al., 1992) mounted on a towed submersible vehicle, MESSOR (Knutsen et al., 2013), constitute the main body of data used in this analysis.

2.1. Plankton net sampling

At total of 43 stations (Fig. 1) was sampled with a WP2 (Fraser, 1966) plankton net (0.25 m^2 mouth opening area, 180 μm mesh) hauled vertically from 200 to 0 m with a vertical haul speed of 0.5 m per second. All samples were split with a Motoda splitter (Motoda, 1959) and one half was preserved in 4% buffered formalin. The other half (or less depending on the amount of biological material present), was fractionated into 3 size groups using sieves (180–1000 μm, 1000–2000 μm and >2000 μm). The two smaller size fractions were rinsed in fresh water, before being transferred to pre-weighed aluminium dishes and dried at 60 °C and weighed in the laboratory on land (Melle et al., 2014). The organisms in the >2000 μm size fraction were rinsed in fresh water before being identified to species and counted. Some taxa were also length measured before being placed on separate aluminium dishes for drying and subsequent weighing. See Melle et al. (2004) for further details about onboard sample processing.

A 1 m^2 opening MOCNESS (Multiple Opening and Closing Net and

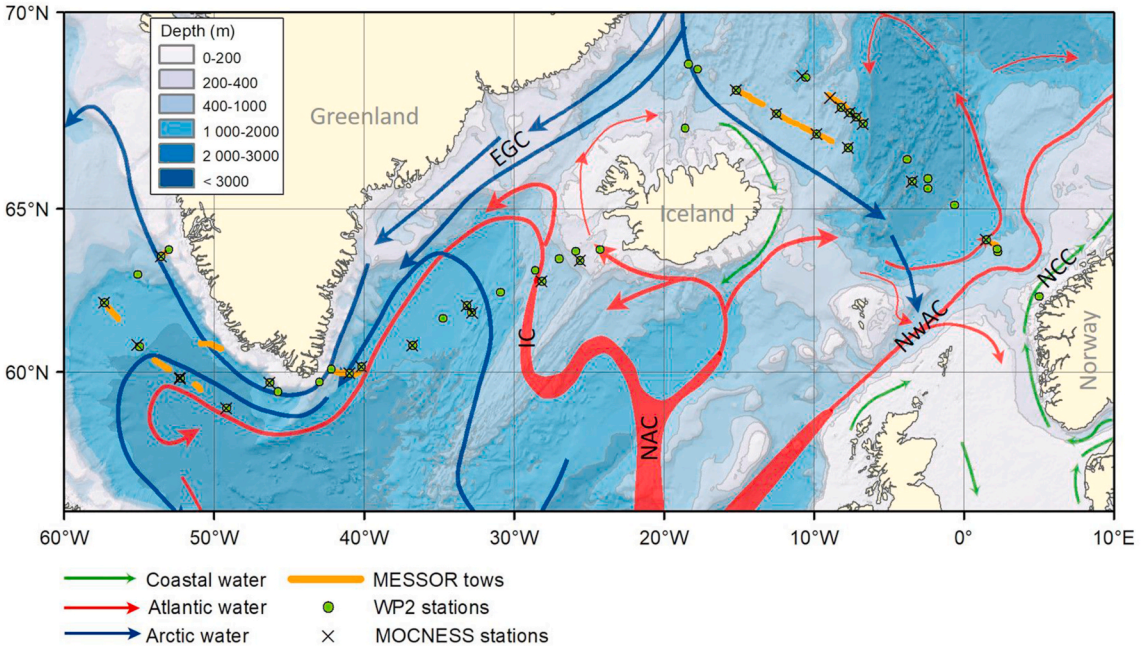

Fig. 1. Locations of stations during the 2013 Euro-BASIN cruise. Green dots denote stations with deployments of WP2 nets 0–200 m, + signs are stations with MOCNESS deployments (0–1000 m), and orange dots show locations of towed vehicle deployments. Current arrows are modified from Knutsen et al. (2017). (For interpretation of the references to color in this figure legend, the reader is referred to the Web version of this article.)

Environmental Sensing System) with a mesh size of 180 µm was used to collect depth stratified samples from the four basins. The MOCNESS was deployed obliquely, sampling the standardised intervals 1000-800, 800-600, 600-400, 400-200, 200-100, 100-50, 50-25 and 25-0 m, thus covering the mesopelagic and epipelagic domains. Samples from the different depth strata were basically treated as described for the WP2 net, but a substantial portion of the hauls were not examined for biomass, only species composition. There was a total of 25 MOCNESS stations (Fig. 1). 23 of the 25 MOCNESS stations were taken during daytime (sun above the horizon), and although all 25 stations are used in the following analyses, the vertical distribution patterns must be considered mainly daytime distributions. For basin-wide comparison of vertical distribution, the weighted mean depth (WMD, m) of each MOCNESS was calculated for each taxonomic species/group and stage (*j*) where this was determined:

$$WMD_j = \frac{\sum_{i=1}^{n} D_i * N_{ji}}{\sum_{i=1}^{n} N_{ji}} \quad 1$$

where *i* is MOCNESS net, D_i is the mean depth (m) of each MOCNESS sample and N_{ji} is the total number of individuals within a sampled depth range sampled, calculated as the density (ind. m^{-3}) of species *j* multiplied with the depth range (m) of MOCNESS net *i*. MOCNESS hauls where no individuals of any group/species/stage where not found in either nets are omitted from further analysis.

C. finmarchius and *C. glacialis* are morphologically very similar and are in the current data distinguish by individual size within developmental stage. Recent studies have indicated that this may lead to erroneous classification of the two species, due to overlap in the size-distributions within stages (Lindeque et al., 2006; Parent et al., 2011; Gabrielsen et al., 2012; Choquet et al., 2018). Since a reanalysis of the formalin fixated material from the cruise, either genetically or by discrimination of antenna coloration on live material (Nielsen et al., 2014) it is unfeasible at present, care should be taken when concluding on the separation of *C. finmarchicus* and *C. glacialis*.

2.2. *In situ* mesozooplankton and particle observations

The OPC (Herman, 1992) and VPR (Davis et al., 1992) mounted on a tow-body (MESSOR; Knutsen et al., 2013) provided data on *in situ* distribution of particles and plankton between some of the stations (Fig. 1). During deployment, the towed vehicle was continually tow-yo'ed between 10 and, usually, 400 m. Whereas the VPR is effectively an underwater microscope, providing dark-field imagery of particles observed in a defined volume (about 150 mL at the settings used, image rate up to 15 Hz), the OPC counts and estimates *in situ* particle sizes passing through its sampling tunnel (opening area ~50 cm^2). At the settings used, the VPR has a pixel resolution of about 24 µm, whereas the OPC is nominally capable of resolving particles down to a size of about 250 µm. Total observation volume for the OPC was assessed by multiplying the opening area of the sampling tunnel with flow estimated from a mechanical flowmeter mounted on the towed body (Knutsen et al., 2013). For the VPR the volume observed per image was estimated based on a factory calibration for the settings used for image extraction, and volumetric densities and coarse identification of particles was done using Visual Plankton (Davis et al., 2005; Melle et al., this issue). The deployments were not equally spread out, due to a combination of time constraints and unfavourable weather (Fig. 1), which is why we have few data available from the Norwegian Sea. The deployments in the Irminger Sea were close to the coast of Greenland, in an area where average fluorescence values from both the underway sampling system and the towed body had quite high values compared to values observed elsewhere in the Irminger Sea during the cruise.

The OPC counts and measures all particles entering the sampling tunnel (Herman, 1992). On the lower end of the size spectrum the OPC is likely to underestimate densities (a function of size and optical transparency), whereas in the higher end of the size spectrum interactions between the sampling tunnel and the particles (either breakage or avoidance of the 2 cm wide by 25 cm high tunnel opening) is likely to bias measurement. In combination with lower densities of larger particles this puts an effective upper limit on what sizes of particles can be measured. Additionally, the range of observable densities can be restricted by particle densities, when the density of particles is high, the

probability of counting multiple non-separable particles as one ("coincident counts") in the observation volume (50 cm^2 × 0.4 cm, Herman, 1992) increases. In practice an upper limit to "measurable" densities of ~10^4 particles m^{-3} has been estimated (Herman et al., 2004), but this limit will also depend on the average size of particles, with larger particles imposing a lower limit.

From the OPC estimates of particle equivalent spherical diameter (ESD) we calculated biovolume for the particles by assuming an prolate spheroid shape (Herman, 1992), assuming that the ESD corresponded to the length of the major axis of ESD, with a minor axis of 1/3 ESD. We calculated relative change in particle densities between day and night as the ratio between night densities and the average of day and night densities, whereas the difference between day and night was calculated as the simple difference between night and day density for a size and depth bin. The OPC is not capable of separating between different types of particles so counts of i.e. zooplankton cannot be separated from for example marine snow or large phytoplankton. Especially in the Irminger and Labrador Seas, the imagery from the VPR documented large amounts of aggregates of algae and marine snow.

2.3. Estimation of biomass from abundance data

In order to make an estimate of species contribution to mesozooplankton biomass, as well the vertical distribution of biomass, data from literature on species and stage prosome length was compiled (Table 1) for the majority of the numerically abundant species (Fig. 5) present in the four basins. Several equations for the allometric relationship between individual body mass and prosome length in copepods and mesozooplankton exists, and here the general relationship from Peters (1983), as suggested by Richardson et al. (2006), is used:

$$W = 0.08 \cdot L_p^{2.1} \quad .2$$

where W is calculated individual wet weight (mg) and L_p is prosome length (mm).

2.4. Environmental data

The fluorescence sensors on both the CTD and on the tow-body show large interregional variations in peak chlorophyll, with values spanning at least 1 order of magnitude, with the exception of the Irminger Sea, where only the data from the tow-body sensor spans this range. The per area average was highest in the western areas, with both sensors showing the lowest values in the Norwegian Sea. The vertical distribution of the fluorescence also varies between the areas, with high values only encountered in the upper 100 m in the eastern basins. In the western basins, moderately high values were also encountered between 100 and 200 m, especially in the Labrador Sea. In the Labrador Sea, fluorescence values above 0.3 were encountered all the way down to ~400 m, for both sensors.

3. Results

3.1. Biomass and species composition

The highest biomass in the 0–200 m WP2 samples was found in the Iceland Sea, with an average of 5.6 g DW m^{-2} (Fig. 2). The lowest average biomass was found in the Labrador Sea, 3.3 g DW m^{-2}. The Norwegian and Irminger Seas had intermediate levels of total zooplankton biomass, between 4 and 5 g DW m^{-2}. However, no basin had significantly more or less total biomass than others (Table 2). In the Iceland Sea, the 3 size fractions (180–1000 μm, 1000–2000 μm, and larger than 2000 μm), contributed roughly equally to the total biomass (Fig. 2). In the Irminger Sea, the 1000–2000 μm fraction was the largest contributor to overall biomass, whereas in both the Labrador and Norwegian Seas the smallest fraction was the dominant. The biomass of the 180–1000 μm fraction was highest in the Norwegian Sea (2.8 g DW m^{-2}); in the 3 other areas biomasses for this fraction were less than 2.1 g DW m^{-2} (Fig. 2). In the 1000–2000 μm size faction, the largest biomass was found in the Irminger Sea (2.3 g DW m^{-2}), where it constituted more than 50% of the total biomass. Biomass of this fraction was a little below 2 g DW m^{-2} in both the Norwegian and Iceland Seas, and below 1 g DW m^{-2} in the Labrador Sea. Overall the biomass found in the larger than 2000 μm size fraction was highest in the Iceland Sea (1.77 g DW m^{-2}), a factor of 3–8 times larger compared to the other areas. There were no significant differences between basins for the two smaller size fractions, but the Iceland Sea had significantly more biomass in the larger size fraction than any other basin (Table 2).

The high biomass found in the largest fraction in the WP2 0–200 m nets in the Iceland Sea was driven primarily by high biomass of *C. hyperboreus* (47%) and Chaetognaths (39%), though also biomass of amphipods and krill contributed (Fig. 3). In the Irminger and Labrador Seas the largest fraction contained relatively high amounts of *Paraeuchaeta* (27% and 19%, respectively) and Chaetognaths (32 and 47%, respectively). Krill did not constitute a dominating part of the large fraction in any basin, with a maximum value of 11% in the Labrador Sea. The spatial distribution of the biomasses suggests a pattern of high biomass in the smallest fraction in areas close to or on the shelves (Fig. 4), with the lowest biomasses consistently registered in offshore areas. Using bottom depth at the WP2 stations as a proxy for shelf vs. basin, a two-sided Spearman correlation test on all WP2 data indeed showed significantly less biomass of the smallest size-fraction in basin areas compared to shelf areas ($p = 0.0068$). However, running the same test on each basin, only the Irminger Sea had a statistically significant correlation ($p = 0.0006$), but the same trend was found for all basins.

The mean value of vertically integrated data from the MOCNESS show that 9 taxa account for the 5 most, in average, numerically dominant species/groups in all basins, with *Oithona* spp. being the most

Table 1
Assigned prosome lengths (mm) for estimation of biomass from abundance data. 1 = Skjoldal et al. (2013), 2 = Madsen et al. (2001), 3 = Conway (2006), 4 = McLaren et al. (1988). * denotes our decision on what stage to assume in the biomass estimation, as the MOCNESS data does not contain information on stage for these species/groups.

Species	CI–CIII	CIV-CV	CVIf	CVIm	larva			Reference
Pseudocalanus spp.	0.54	0.87	0.86	0.82				1
Paraeuchaeta spp.	1.30	3.07	6.10	4.40				1,3
Metridia spp.	1.09	1.55	2.37	1.69				1
Cirripedia					0.55			1
Oithona spp.		0.77						1*
Oncaea spp.			0.68					1*
Microcalanus pusillus		0.43						1*
	CI	**CII**	**CIII**	**CIV**	**CV**	**CVIf**	**CVIm**	
Calanus hyperboreus	1.19	1.69	2.45	3.41	4.20	6.80	6.80	4,2
Calanus glacialis	0.89	1.31	1.74	2.48	3.31	3.55	3.55	4,2
Calanus finmarchicus	0.66	0.96	1.35	1.85	2.45	2.56	2.40	1

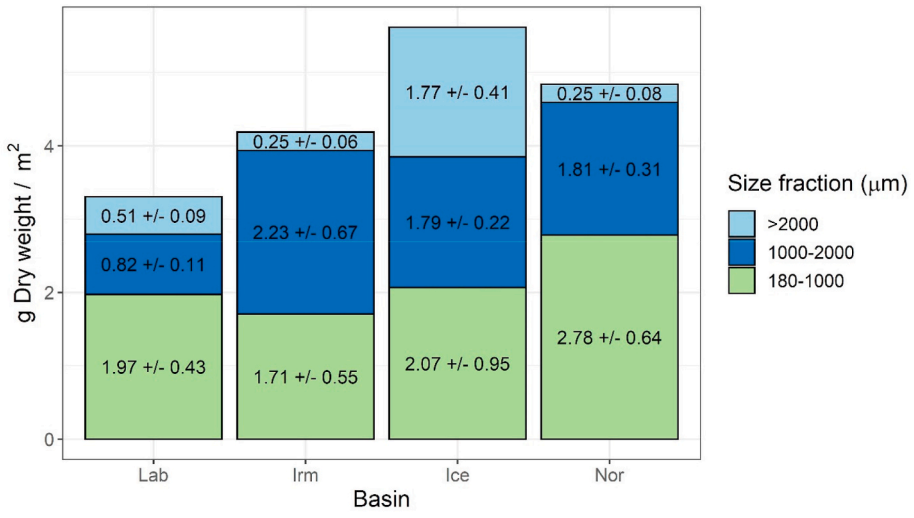

Fig. 2. Average dry-weight (g DW m^{-2}) ± standard error of fractionated zooplankton biomass samples from WP2 nets 0–200 m.

Table 2
P-values from ANOVA comparing measured dry weight biomass between all basins and size fractions/groups. Significant differences ($p < 0.05$) denoted by *.

Size fraction/ group	Compared basins					
	Ice-Nor	Irm-Ice	Irm-Nor	Lab-Ice	Lab-Irm	Lab-Nor
Total biomass	0.91	0.58	0.93	0.29	0.88	0.62
180–1000 µm	0.88	0.97	0.63	0.99	0.99	0.86
1000–2000 µm	0.99	0.90	0.91	0.57	0.20	0.53
>2000 µm	0.00003*	0.00001*	1.00	0.00136*	0.81	0.82
C. hyperborues	0.00003*	0.00001*	0.99	0.00012*	0.99	0.99
Chaetognatha	0.00003*	0.00005*	0.94	0.01098*	0.60	0.35
Pareuchaeta	0.98	0.56	0.34	0.33	0.92	0.18
Krill	0.49	0.60	0.99	0.93	0.94	0.87
Amphipoda	0.35	0.17	0.98	0.24	0.99	0.98

abundant (likely under sampled – see discussion) across all basins (Fig. 5). *C. finmarchicus* (stages CI-CVI) was the second most common species numerically in all basins, except in the Iceland Sea where it appeared that *Oncaea* spp. was the second most common group. Cirripedia larva was generally only found small numbers, except for one station, near shore close to Nuuk, Greenland, in the Labrador Sea. Members of the Larvacea group were common only in the Labrador Sea. Ostracods, *Pseudocalanus* spp. and *Microcalanus* spp. were registered in all basins.

3.2. Vertical distribution and stage development

A general observation on the vertical distribution of mesozooplankton shows that the Norwegian and Iceland Seas appear have a shallower distribution compared to what was observed in the Labrador and Irminger Seas (Fig. 6). For numerical comparison of the basins, we estimated the weighted mean depth (WMD; Table 3; Eq. (1)). The pattern of shallower vertical distribution in the Norwegian basin is primarily driven by the vertical distribution of *Oithona* spp. with an WMD of 32 m in the Norwegian Seas, while this numerous copepod had deeper WMD's in the Labrador (102m) and Irminger Sea (87m).

For *C. finmarchicus*, the highest densities of individuals were found in the upper 25 m in the Labrador ($p < 0.03$), Irminger ($p < 0.0006$) and Iceland ($p < 0.0003$) Seas (Fig. 7), albeit not in the Norwegian Sea, when comparing all depth intervals against each other (one-way Anova). Younger stages appear to in general have shallower WMDs than older stages (Table 3). The weighted mean depth of *C. finmarchicus* stage CV was found at 119, 121, 59 and 73 m in the Labrador, Irminger, Iceland and Norwegian basins respectively. The stage composition of *C. finmarchicus* varied distinctly between basins (Fig. 7). In the Norwegian and Labrador Seas, younger stages (CI–CIV) were more dominant compared to the Iceland and Irminger Seas where stages CV and CVI composed more than 50% of the total number of *C. finmarchicus*.

The Labrador Sea was the only place where *C. glacialis* occurred in numbers indicating the existence of a thriving population. *C. glacialis* were not found at all in the Irminger Sea, and only in small numbers at shallow depths in the Norwegian and Iceland Seas (Fig. 7). In the Iceland Sea, developmental stage CI was the only stage present, while early stages (CI–CIII) constituted more than 50% of the individuals in the Labrador Sea.

The highest densities of *C. hyperboreus* were found in the Labrador Sea within the upper 50 m and stage CI (WMD = 30) and CII (WMD = 21) accounted for more than 75% of the total numbers. In the Iceland and Norwegian Seas, older stages (CIV+) made up the majority of individuals (Fig. 7). The occurrence of *C. hyperboreus* was very low in the Irminger Sea. Older stages (CV+) had a WMD below 150 m in all basins.

In terms of contributions to biomass of the large size fraction (>2 mm), chaetognaths were a major contributor in the Iceland Sea in the upper 200 m (Fig. 3), with very little contribution in the Norwegian Sea. However, in terms of numerical abundance, chaetognaths were found in relatively high numbers in both the Norwegian and Iceland Seas, with an average density of around 17 (Nor) and 8 (Ice) individuals m^{-3} in the upper 25 m. The general trend showed a decreasing density with increasing depth with a weighted mean depth of between 181 and 284 in all basins. Chaetognaths appeared to be less numerically important in the Labrador and Irminger basins compared to the to eastern basins.

Oncaea spp. was distributed throughout the water column (Fig. 6) in low numbers in the two western basins, while in the Norwegian Sea members of this genus were found mainly in the upper 200 m (WMD = 108m). In the Iceland Sea, the vertical density distribution was bimodal with one peak at the surface, a second one between 400-600m depth, and an overall WMD of 282 m.

No significant differences were detected between basins in surface integrated densities of the of males or females of carnivorous copepod *Paraeuchaeta* spp. There were however significantly more individuals of stage CIV-CV in the Labrador and Irminger basins compared to the Norwegian and Iceland seas (Anova; Ice-Lab: $p = 0.0002$, Ice-Irm: $p = 0.0003$, Nor-Lab: $p = 0.007$, Nor-Irm: $p = 0.01$). The mean vertical distribution in density (ind. m^{-3}) of stages CI–CIII and CIV-CV combined, indicate a peak at 25–50m in the Norwegian Sea, 50–100m in the Irminger Sea and 100–200 m in the Labrador Sea. In the Iceland Sea, no clear vertical distribution pattern was seen for theses stages. CVI femals

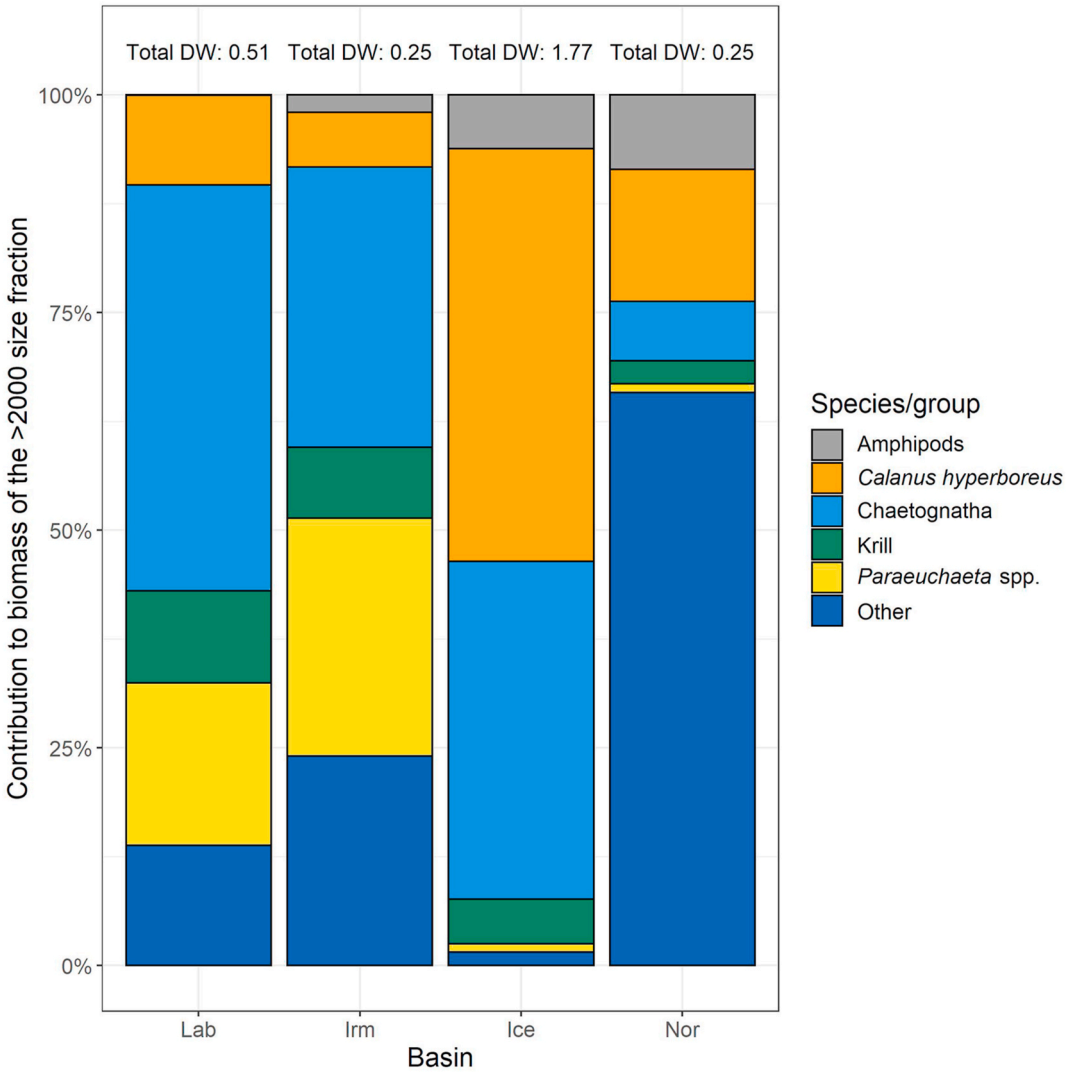

Fig. 3. Taxonomic composition of the >2000 μm size fraction (% of total) in the 0–200 m WP2 nets in the four basins. Number on top of columns show the basin specific average total biomass (g DW m^{-2}). The "Other" group contains what remains on the 2000 μm sieve after removing the other taxa, including fish and larger jellies (not shown).

appears to be distributed deepest in the Norwegian (WMD = 468) and Icelandic Seas (WMD = 455), somewhat shallower in the Irminger Sea (WMD = 354) and most shallow (WMD = 251) in the Labrador Sea.

Pseudocalanus spp. appeared to be most abundant in the Iceland and Norwegian Seas with CVI females being the most common stage (Fig. 8). This was however only significant when comparing the Iceland Sea to the Irminger ($p = 0.003$) and Labrador ($p = 0.006$) basins. The weighted mean depth of this stage was deeper, but not significantly, in the Iceland Sea (WMD = 132m) compared to the Norwegian Sea (WMD = 59m). The density of younger stages (CI–CIII and CIV-CV) peaked in the upper 25m in the Iceland and Labrador Seas and the upper 50m in the Norwegian Sea (Fig. 8). *Pseudocalanus* spp. were rare in the Irminger Sea.

3.3. *Calanus finmarchicus* phenology

The stage distribution of *C. finmarchicus* on the westward and eastward surveys of the four seas are shown in Fig. 9. At the two first stations in the Norwegian Sea we observed many CI–CIII, few CIV and more CV-CVI. This was interpreted as the overwintering generation (G0), still being present in stages CV-CVI while the new generation (G1) had recruited to the three youngest copepodite stages, CI–CIII. In the Iceland and Irminger Seas, G0 dominated the population on the westward survey, although some G1 were present in the Irminger Sea in low numbers (CI–CIII). When entering the Labrador Sea, the first two stations were close to the West-Greenland shelf and most of the populations were already in G1, although some individuals of the G0 remained in stages CV and CVI. On the eastward leg, the central parts of the Labrador Sea were surveyed and stage distribution there seemed to be a mix of G0 and G1, like near the Greenland shelf, but with fewer young stages of G1. Some young stages of G1 were present in the Irminger Sea during the eastward survey. In the Iceland Sea and the three western stations in the Norwegian Sea, G0 still dominated the population. The last station much closer to the Norwegian shelf where we observed active recruitment to G1 on the westward leg some young stages still lingered, but the population was dominated by older stages, presumably belonging to G1.

The relationship between the number of *C. finmarchicus* of stages CV-CVI and the depletion of nitrate during the bloom development (Naustvoll et al., this issue) is shown in Fig. 10. These stages mainly represented the G0 as described above. While nitrate was depleted from the mixed layer, the number of CV-CVI diminished. When about 0.2 mol m^{-2} were used, few CV-CVI of the G0 were left.

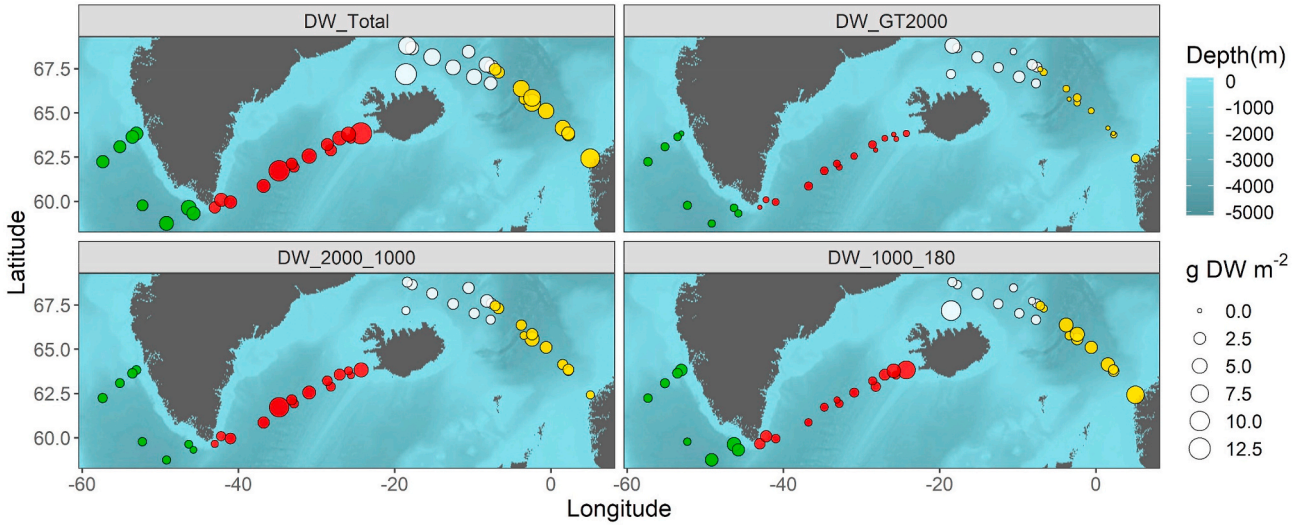

Fig. 4. Spatial distribution of average dry weight (g DW m^{-2}) of the three size fractions from the 0–200 m WP2 samples. Coloured symbols denote stations assigned to the different basins. Green: Labrador Sea, Red: Irminger Sea, White: Iceland Sea, Yellow: Norwegian Sea. (For interpretation of the references to color in this figure legend, the reader is referred to the Web version of this article.)

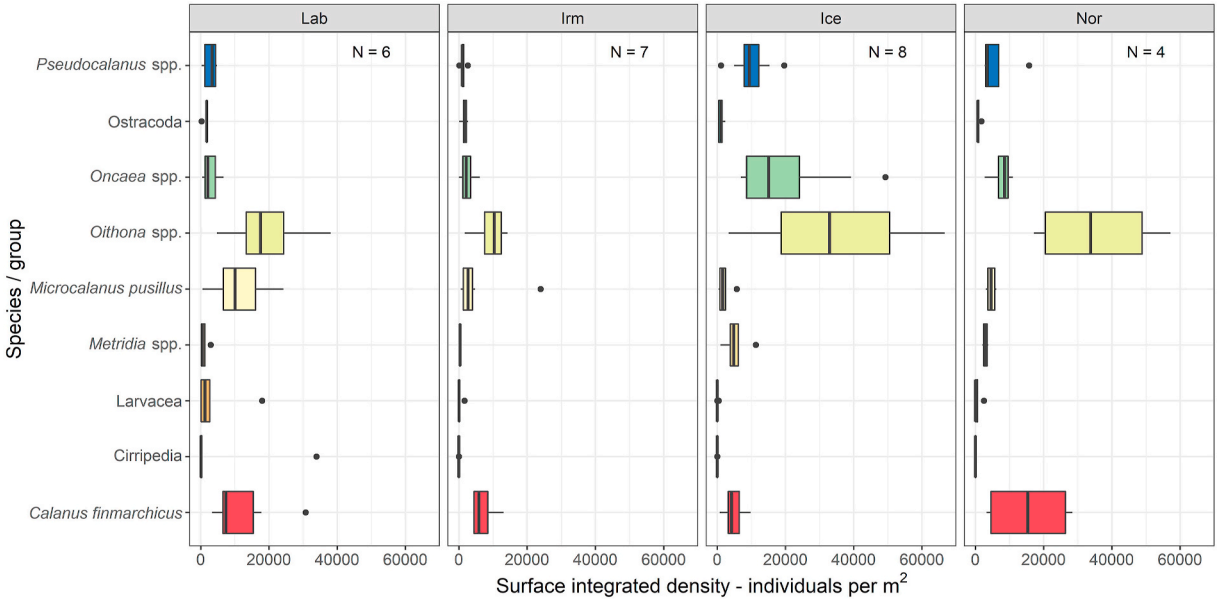

Fig. 5. Boxplot of the numerical abundance of the most common species. Nine taxa account for the 5 most numerically dominant species/groups across all investigated basins. All stages included. *Oithona* spp. was the most common genus in all basins.

3.4. Optical plankton counter

The highest average particle density per 25 m interval (e.g. sum of all sizes), was registered in the Norwegian Sea (daytime, 25–50 m, ~7600 m^{-3}). In the Labrador and Irminger Seas, total estimated particle densities in the upper 50m were lower (peak ~5600 m^{-3}), but the particle densities peaked at intermediate sizes (1–3 mm) (Fig. 11). As a consequence, the biovolume estimated by the OPC in the Labrador Sea was more than 3 times greater than in the Norwegian and Iceland Seas in the upper 200 m (Fig. 12 A1-4). To make the OPC data more comparable with the WP2 data, we split the biovolume measurements into different size-fractions (Table 4), based on ESD. Compared to the Norwegian and Iceland Seas, the two western basins had higher total biovolumes (two sided Mann-Whitney *U* test of daytime biovolumes for particles in the size range 0.3–5 mm integrated from 20 to 180 m per MESSOR cast, N = 41/42, W = 1612, p « 0.001), as well as larger average particle sizes (two sided Mann-Whitney *U* test of daytime weighted average size of particles in the size range 0.3–5 mm, integrated from 20 to 180 m per MESSOR cast, N cast = 41/42, W = 1624, p « 0.001) and thereby a higher proportion of biovolume in the larger ESD classes (see Fig. 12 A1-4 and Table 4).

In all areas there were differences in the particle densities estimated between day and night (Fig. 12 B1-4). In the eastern basins, densities of particles in the range ~0.63–~1.6 mm ESD had reduced densities at depth during night-time compared to during day (Fig. 12 B1-4). In the Irminger and Norwegian Seas, biovolumes of particles in the size range of ~1–2.5 mm ESD increased strongly close to the surface during night-time (Fig. 12 C2, C4). To summarise estimates of biovolume changes over the diel cycle (Fig. 12 C1–C4), we integrated the biovolume of particles in the size range 0.5–2.5 mm ESD day and night (Fig. 12 D1-D4). In the two eastern basins, biovolumes estimated deeper than 100 m during night-time were on average lower than those found during

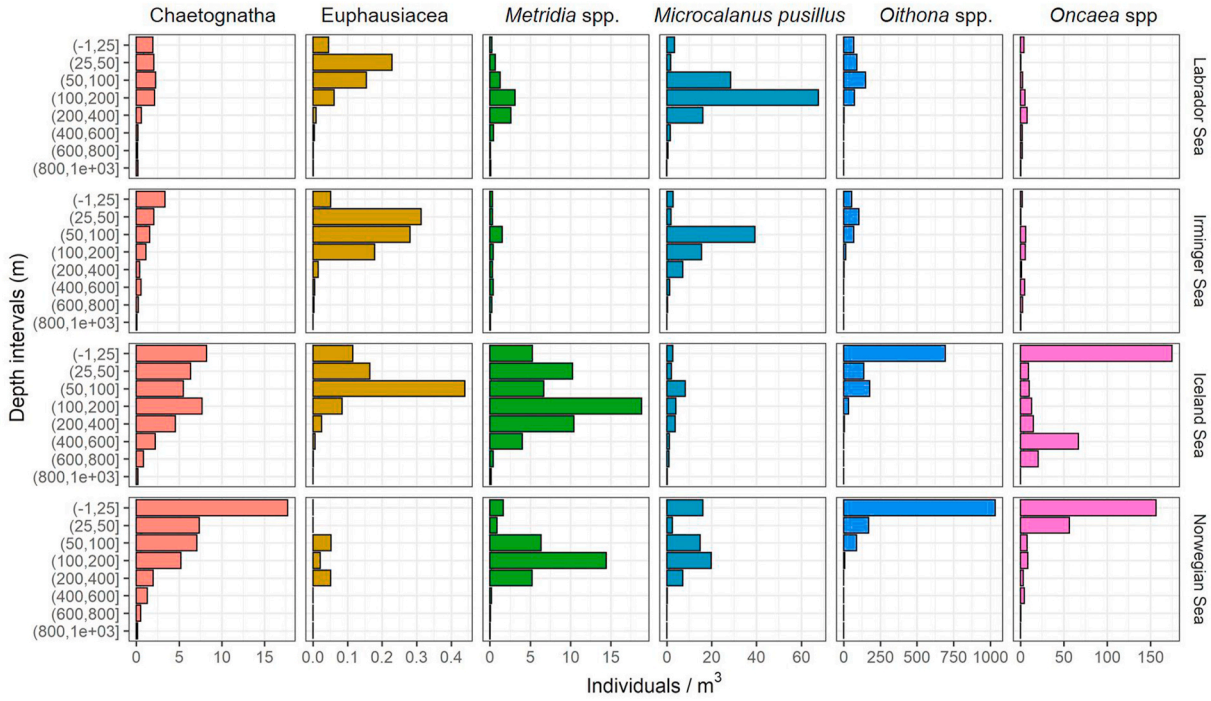

Fig. 6. Vertical distribution of numerically common groups (all stages). The vertical resolution corresponds with the depth intervals used for the MOCNESS.

daytime, whereas in the western basins biovolumes estimated deeper than 100 m was higher during night-time (Fig. 12 C1–C4, D1-D4). The magnitude of differences varied between depths and areas, with the highest drop in biovolume during night-time found in the Irminger and Labrador Seas, in the depth range 30–80 m (Fig. 12 D1-D4).

3.5. Video plankton recorder

The images from the video plankton recorder (VPR) were sorted into 5 categories, Copepods, *Pseudocalanus* females with eggs, gelatinous organisms, primary producers (aggregates of algae) and marine snow. Based on the categorization (Melle et al., this issue) and the observation volume of the VPR, densities of the different categories were calculated for the different areas and depth strata (Fig. 13). For the Norwegian Sea, the dataset was limited (only 3.5 h sampling time). In the Irminger and Iceland Seas the highest copepod densities were registered in the upper 200 m, whereas in the Labrador Sea, the highest average copepod densities were registered at depth (Fig. 13). Estimated densities of gelatinous organisms were at least an order of magnitude higher in the Labrador and Irminger Seas than in the Iceland Sea. In the western basins, especially the coastal areas of the Labrador Sea, the VPR also registered high amounts of primary producers in the form of algae and aggregates of algae. The densities of the aggregates peaked close to the surface. Marine snow occurred in all basins, at all depths, densities peaking at about 100m. Estimated densities were highest in the western basins (Fig. 13).

3.6. Estimation of biomass from abundance data

In terms of numerical abundance, species/stages with small prosome lengths (0–1 mm) dominated the samples in all basins (Fig. 14A), with *Oithona* spp. being on average the most common species in the (0.75–1.0 mm) prosome length bin group. In the smallest length bin, *Microcalanus pusillus*, *Oncaea* spp. and *C. finmarchius* stage CI (see Table 1) were common. In addition, Cirripedia larva occurred in this bin in the Labrador Sea.

The estimated biomass based on prosome length, showed a distinctly different pattern when compared to the numerical abundance. Where small species/stages dominated numerically, the biomass distribution based on prosome length showed bimodal distribution (Fig. 14B), and in the case of the Iceland Sea, a multimodal distribution. The first biomass peak at 0.75–1.0 mm prosome length, apparent in all basins, were made up from *Oithona* spp., *Pseudocalanus* spp. and *C. finmarchicus* stage CII. The second peak, at 2.0–2.5 mm prosome length in the Iceland Sea and at 2.5–3.0 mm in the Labrador, Irminger and Norwegian Seas, were composed primarily by *C. finmarchicus* stage CV and CVI. However, in the Iceland Sea, and to a lesser extent the Norwegian Sea, *Metridia* spp. appeared to also play an important part of the biomass within this bin range. The third peak, clearly visible only on the Iceland Sea, were made up from older stages of *C. hyperboreus*.

Overall, the majority of the biomass were located above 200 m, but the average values were different between basins (Fig. 14C, red lines) and also between length groups (Fig. 14C, bars). The Labrador and Irminger Seas appeared to have the shallowest distributed biomass, with more than 80% of biomass found above 200m. In the Iceland Sea, the distribution seemed deeper with 36% of the biomass found below 200m.

3.7. Environmental data

The fluorescence sensors on both the CTD and on the tow-body show large interregional variations in peak chlorophyll, with values spanning at least 1 order of magnitude, with the exception of the Irminger Sea, where only the data from the tow-body sensor spans this range. The per area average was highest in the western areas, with both sensors showing the lowest values in the Norwegian Sea. The vertical distribution of the fluorescence also varies between the areas, with high values only encountered in the upper 100 m in the eastern basins. In the western basins, moderately high values were also encountered between 100 and 200 m, especially in the Labrador Sea. In the Labrador Sea, fluorescence values above 0.3 were encountered all the way down to ~400 m, for both sensors.

4. Discussion

In terms of biomass in the upper 200 m, we found no significant differences in size fractionated biomass the 180–1000 and 1000–2000

Table 3
WMD (m) ± SD of dominant species/groups and stages in the 4 surveyed North Atlantic basins based on MOCNESS samples. Number in parenthesis denotes number of profiles with valid calculation of WMD, and thus (0) means no observations, (1) mean one profile with data and hence no SD.

Species/Group	Stage	Lab	Irm	Ice	Nor
Calanus finmarchicus	CI	25 ± 10 (6)	17 ± 7 (7)	27 ± 12 (7)	19 ± 5 (4)
Calanus finmarchicus	CII	27 ± 10 (6)	17 ± 6 (7)	98 ± 166 (8)	19 ± 5 (4)
Calanus finmarchicus	CIII	29 ± 15 (6)	23 ± 12 (7)	41 ± 39 (8)	18 ± 4 (4)
Calanus finmarchicus	CIV	49 ± 23 (6)	40 ± 18 (7)	61 ± 46 (8)	27 ± 15 (4)
Calanus finmarchicus	CV	119 ± 72 (6)	121 ± 57 (7)	59 ± 35 (8)	73 ± 18 (4)
Calanus finmarchicus	CVI female	44 ± 21 (6)	38 ± 20 (7)	49 ± 34 (8)	43 ± 11 (4)
Calanus finmarchicus	CVI male	87 ± 34 (6)	72 ± 74 (7)	110 ± 68 (8)	63 ± 31 (4)
Calanus glacialis	CI	28 ± 15 (3)	(0)	13 (1)	13 (1)
Calanus glacialis	CII	33 ± 35 (4)	(0)	13 (1)	13 (1)
Calanus glacialis	CIII	121 ± 212 (5)	38 (1)	239 ± 210 (4)	13 ± 0 (2)
Calanus glacialis	CIV	51 ± 66 (4)	292 ± 360 (2)	243 ± 243 (8)	(0)
Calanus glacialis	CV	88 ± 63 (4)	(0)	171 ± 127 (5)	75 (1)
Calanus glacialis	CVI female	215 ± 116 (5)	372 ± 225 (4)	156 ± 109 (8)	300 ± 0 (2)
Calanus glacialis	CVI male	118 ± 39 (3)	75 (1)	265 ± 157 (3)	(0)
Calanus hyperboreus	CI	30 ± 10 (5)	13 (1)	400 ± 141 (2)	17 ± 3 (2)
Calanus hyperboreus	CII	21 ± 4 (5)	13 (1)	21 ± 14 (3)	279 ± 455 (3)
Calanus hyperboreus	CIII	96 ± 26 (6)	312 ± 168 (3)	160 ± 115 (7)	69 ± 79 (4)
Calanus hyperboreus	CIV	93 ± 36 (6)	224 ± 145 (7)	101 ± 63 (8)	136 ± 75 (4)
Calanus hyperboreus	CV	210 ± 138 (6)	177 ± 183 (7)	163 ± 89 (8)	219 ± 95 (4)
Calanus hyperboreus	CVI female	210 ± 119 (6)	301 ± 143 (7)	273 ± 88 (8)	390 ± 134 (4)
Calanus hyperboreus	CVI male	700 (1)	(0)	498 ± 131 (6)	(0)
Oithona spp.		102 ± 21 (6)	87 ± 26 (7)	81 ± 67 (8)	32 ± 15 (4)
Chaetognatha		222 ± 81 (6)	284 ± 147 (7)	237 ± 83 (7)	181 ± 97 (4)
Metridia spp.		293 ± 141 (6)	364 ± 162 (7)	248 ± 96 (8)	204 ± 46 (4)
Microcalanus pusillus		171 ± 58 (6)	232 ± 83 (7)	270 ± 111 (8)	173 ± 65 (4)
Oncaea spp.		294 ± 115 (6)	383 ± 189 (7)	282 ± 234 (8)	108 ± 55 (4)
Paraeuchaeta spp.	CI–CIII	235 ± 63 (6)	162 ± 28 (7)	358 ± 240 (8)	246 ± 267 (4)
Paraeuchaeta spp.	CIV-CV	191 ± 63 (6)	198 ± 79 (7)	465 ± 227 (8)	248 ± 213 (4)
Paraeuchaeta spp.	CVI female	251 ± 81 (6)	354 ± 50 (7)	455 ± 152 (8)	468 ± 213 (4)
Paraeuchaeta spp.	CVI female w/egg	500 ± 0 (3)	388 ± 102 (3)	528 ± 167 (7)	150 (1)
Paraeuchaeta spp.	CVI male	457 ± 207 (6)	524 ± 132 (7)	480 ± 213 (8)	477 ± 287 (4)
Pseudocalanus spp.	CI–CIII	125 ± 134 (6)	340 ± 166 (7)	52 ± 56 (5)	42 ± 20 (4)
Pseudocalanus spp.	CIV-CV	209 ± 123 (6)	310 ± 110 (7)	197 ± 157 (8)	79 ± 100 (4)
Pseudocalanus spp.	CVI female	252 ± 89 (6)	259 ± 72 (7)	132 ± 107 (8)	59 ± 75 (4)
Pseudocalanus spp.	CVI male	313 ± 231 (5)	352 ± 238 (7)	132 ± 156 (6)	149 ± 149 (4)

µm fractions, but the Iceland Sea had significantly more biomass in the >2000 µm fraction. In terms of numerical abundance, *Oithona* spp. was most common in all basins. The Irminger Sea differed from the others, having fewer copepods, while, in the Labrador Sea, we observed high densities of larvaceans and cirripeds. In terms of biomass, our results are similar to previous studies, which have found the overall biomass in the different regions to consist of only a few dominant species. In the Labrador Sea, three species of *Calanus* complex (*C. finmarchicus, C. glacialis* and *C. hyperboreus)* usually make up > 70% of copepod biomass (Head et al., 2003), with *C. finmarchicus* usually alone making up more than 60% of total biomass and 80% of numbers of large copepods in spring and summer. In the Irminger Sea, *C. glacialis* and *C. hyperboreus* are usually found to be of lesser importance, but five copepod taxa (*C. finmarchicus, Paraeuchaeta norvegica, C. hyperboreus, Oithona* spp. and *Oncaea* spp.) usually constitute more than 95% of total copepod biomass (Gislason, 2003). Gislason and Silva (2012) identified three main mesozooplankton communities in the Subarctic Iceland Sea, "(i) an Atlantic community in the east, with *C. finmarchicus* and *Pseudocalanus* spp. most abundant, (ii) an Arctic community at high latitudes, with large numbers of *C. hyperboreus* and *C. glacialis*, and (iii) a community with coastal affinities at lower latitudes, with large numbers of *Temora longicornis* and *Acartia* spp." As can be seen from our data from the Iceland Sea, most of our samples are similar to community (i) described above. However, older stages (CIV-CV) of *C. hyperboreus* were also present in the Iceland Sea, but with very few younger stages (CI–CIII) present at the time of sampling. In the Labrador Sea, all stages of the Arctic species *C. glacialis* and *C. hyperboreus* were present in some quantities, despite the samples coming from a lower latitude than the Iceland Sea. In the Norwegian Sea, the mesozooplankton community biomass is dominated by the copepods, making up 60–75% during summer and more than 50% year-round (Wiborg, 1954). *C. finmarchicus, Pseudocalanus* spp., *Oithona* spp. and *Oncea* spp. are the most abundant of all species, other taxa being at least an order of magnitude less abundant (Østvedt, 1955). The biomass of *C. finmarchicus* during spring and summer have been found make up more than 80% of the copepod biomass (Wiborg, 1954).

4.1. Basin scale variation in biomass and species abundance observed by net-sampling

The biomass of the smallest size fraction (180–1000 µm) in the upper 200 m of the water column was highest in the Norwegian Sea. When comparing the observed biomass data from the WP2 in the Norwegian Sea with the species and stage abundances from the MOCNESS within the same depth range, it is likely that a significant proportion of the small biomass was *Oithona* spp. and small stages of *C. finmarchicus*. With an adult body length of approximately 500 µm (Castellani et al., 2007), all *Oithona* spp. retained by the 180 µm MOCNESS and subsequently size fractionated, should end up in the 180–1000 µm size category. On the other hand, nauplii stages are probably severely undersampled since their body lengths are less than ~250 µm (Gallienne and Robins, 2001). Unlike *C. finmarchicus*, *Oithona* spp. is active and reproduces year around, and there are thus likely to be individuals of most stages present. In the Irminger Sea, Castellani et al. (2007) reported that of all *Oithona* spp. individuals, 74.9% in spring, 62.6% in summer and 76.9% in winter, were at the naupliar stages. Of the investigated basins, the lowest biomass in the small size fraction was found in the Irminger Sea (1.71 g DW m^{-2}), which had the largest biomass of the middle size faction (1000–2000 µm). Since *Oithona* spp. ends up in the smallest size fraction, it is likely that larger stages of *C. finmarchicus* makes up the majority of biomass in the middle size fraction, considering the stage composition of *C. finmarchicus* in the upper 200 m from the MOCNESS data (Fig. 7).

The biomass of the >2000 µm size fraction in the upper 200 m was higher in the Iceland Sea than in the other basins (Fig. 3.) and was composed mainly of *C. hyperboreus* and chaetognaths. Krill and amphipods also had higher average biomass in the Iceland Sea basin compared to the other three basins. The size structure of zooplankton communities

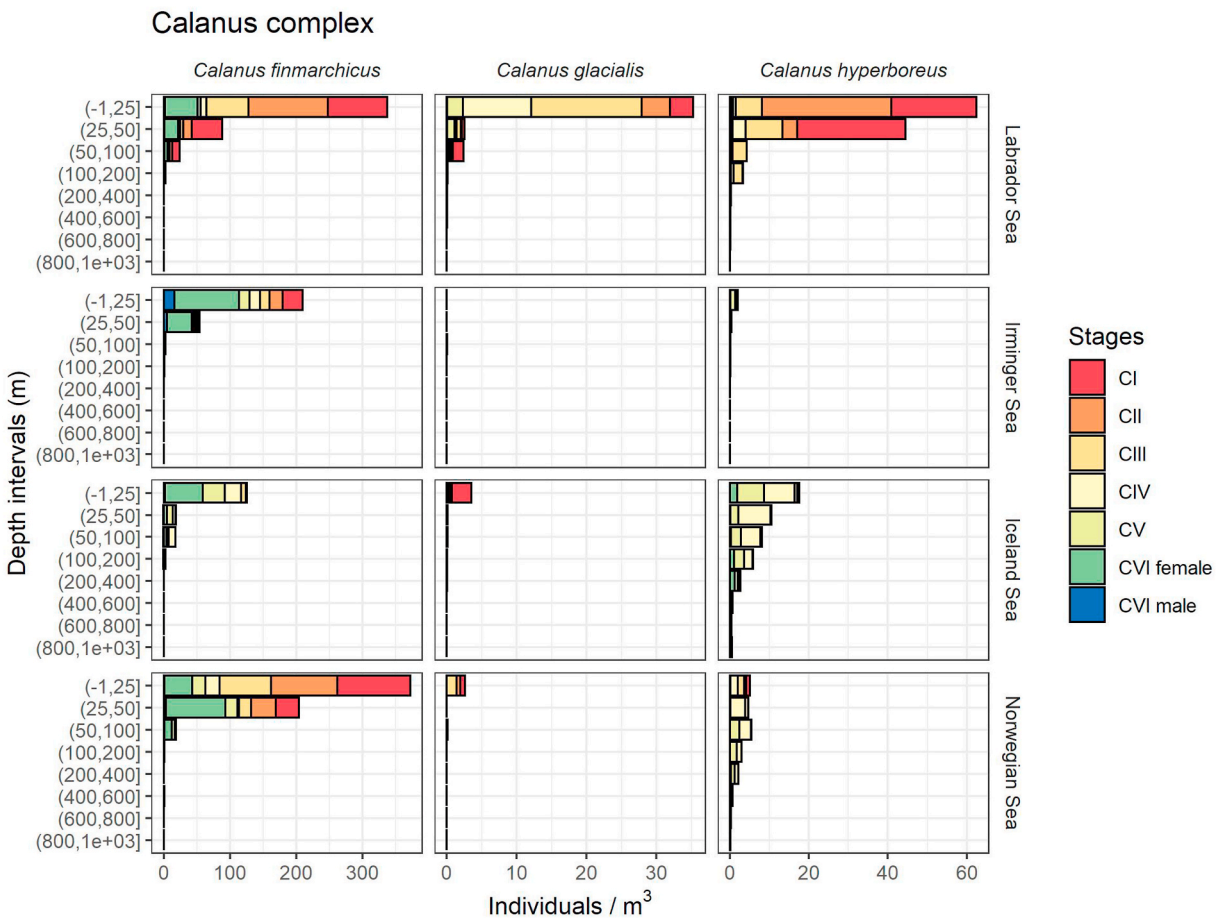

Fig. 7. Vertical distribution of *Calanus* developmental stages. The vertical resolution corresponds with the depth intervals used for the MOCNESS.

is known to be affected by ambient temperature (Martin et al., 2006; Chiba et al., 2015), where cold-water habitats favour larger forms with longer generation times, while smaller sizes and shorter generation times are favoured by warm-water communities. Across the investigated North Atlantic basins, this trend were seen where larger copepod forms such as *C. glacialis* and *C. hyperboreus* were more dominant in water masses influenced by cold Arctic water (Spearman correlation test: log (integrated abundance) ~ temperature; $p = 0.007$ and $p = 0.000003$, respectively). No effect of water temperature was found on the abundance of *C. finmarchicus* ($p = 0.795$) which indicate that all surveyed basins have temperatures that are within optimal range for this species. This study thus substantiates these temperature mediated patterns in abundance variation of these three species of the *Calanus* complex (Broms et al., 2009; Falk-Petersen et al., 2009). However, also other zooplankton groups may show similar patterns. In our data, this is especially clear in the case of chaetognaths when comparing the biomass of chaetognaths large enough to be retained in the >2000 μm size fraction in the WP2 nets (Fig. 3) with the numerical surface integrated densities based on MOCNESS samples within the same depth range (200-0m). The Iceland Sea had a significantly higher biomass of chaetognaths than the Norwegian Sea (Fig. 3, Table 2), but numerically, more individual chaetognaths (Fig. 6) were on average found in the Norwegian Sea (1502 ind. m^{-2}) than the Iceland Sea (1407 ind. m^{-2}). Thus, the cold Iceland Sea is likely to have larger individuals compared to the warmer Norwegian Sea, possibly due to the presence of the large Arctic species *Pseudosagitta maxima* (Kulagin and Neretina, 2017). However, also differences in development could partly explain this pattern, but that cannot be addressed by the current dataset. The same pattern is also suggested when comparing the biomass (Lab = 0.24/Nor = 0.017 g DW m^{-2}) and surface integrated densities of chaetognaths from the cold Labrador Sea (427 ind. m^{-2}) with the Norwegian Sea, even though the difference in biomass is not significantly different (Table 2).

A pattern seen in the biomass data, is the increased biomass in the smallest fraction (180–1000 μm) close to the coast (Fig. 4). Since the pelagic ecology of the basins was the focus of the study, we had relatively few stations close to the coast, and the pattern is therefore primarily driven by high values found at a few stations. On-shelf areas typically have different water-masses than the deeper basins (i.e. East Greenland Current, Icelandic Coastal Current, Norwegian Coastal Current) and the timing of the spring bloom in these areas is likely to be different to that found in the basins. However, the basins covered by the cruise varied from pre-bloom to post-bloom phase (Naustvoll et al., this issue). While not statistically significant in all basins on a per basin test, increased biomasses in the smallest fraction was indicated in all basins, which may suggest that the observed increases were not solely an effect of differences in relation to bloom-timing. Also, it is known that small species of genera like *Pseudocalanus*, *Temora*, *Acartia*, *Centropages* could be abundant in shelf sea waters (Bucklin et al., 2000; Durbin and Kane, 2007; Gislason and Silva, 2012; Staurland Aarbakke et al., 2014), but such regions could also be more subject to freshwater runoff that could host a range of additional small species, like *Podon* and *Evadne* and larvae of benthic invertebrates (cf. Skjoldal et al., 2013), although species phenology will determine which organisms could impact biomass of the smaller size fraction at a given place and time. There are several other possible processes that potentially could contribute to increased coastal biomass in the small fraction, ranging from physical (i.e. temperature driven), to bottom-up (i.e. differences in productivity levels and types of primary producers) and top-down driven (i.e. reduced predation from vertically migrating planktivores (Klevjer et al., this issue b)). A possible coastal-offshore gradient in size distribution of

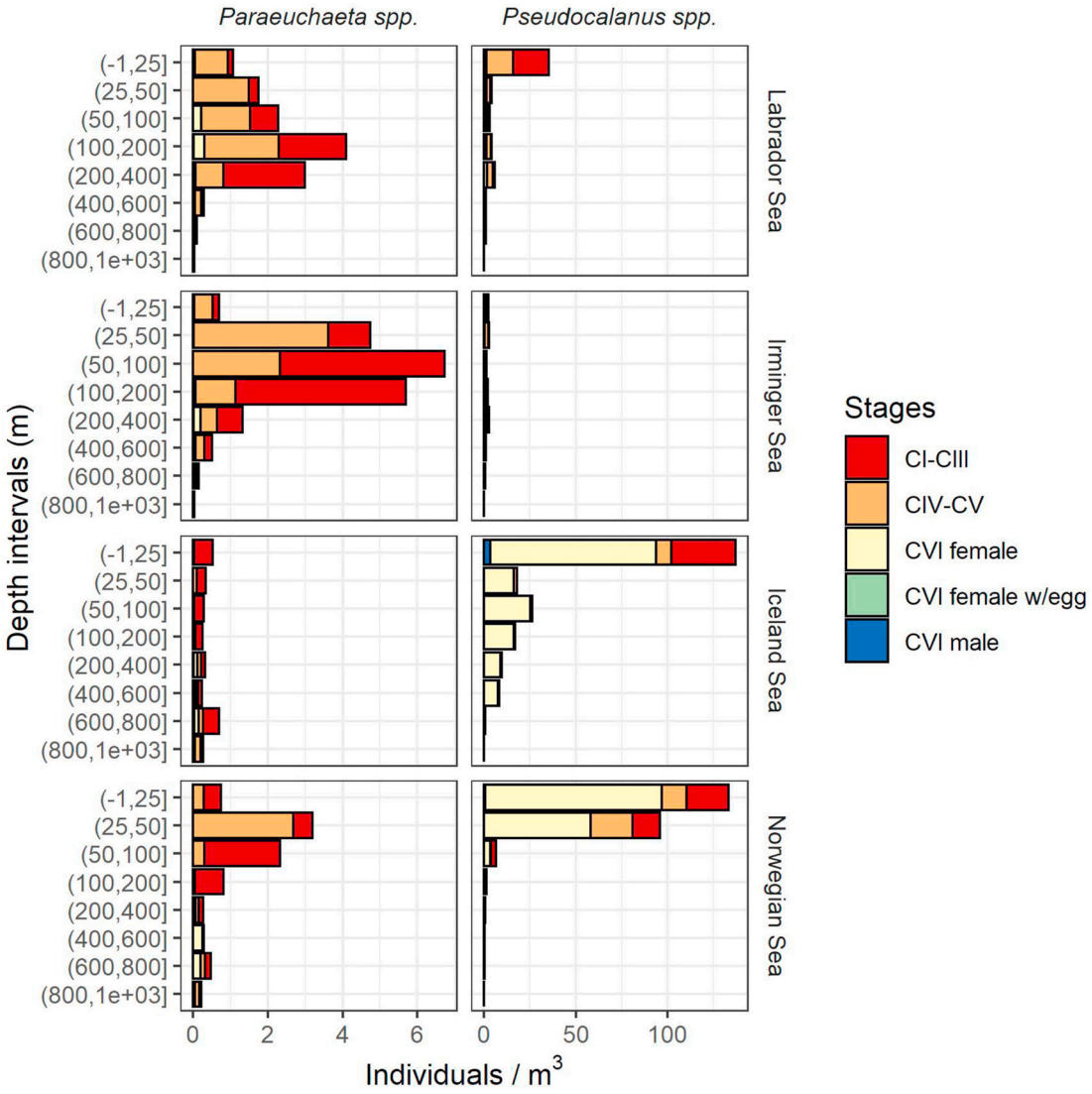

Fig. 8. Vertical distribution of *Paraeuchaeta* spp. and *Pseudocalanus* spp. stages. The vertical resolution corresponds with the depth intervals used for the MOCNESS.

mesozooplankton is an interesting pattern for future studies since such difference is likely to have ecological consequences, but it will require a more specific sampling design than was undertaken on this cruise.

The Norwegian Sea and the Irminger/Labrador Sea Sub-polar Gyre are the core overwintering areas for *C. finmarchicus* in the North Atlantic (Heath et al., 2004), and thus distance from these areas is believed to play an important role in understanding varying abundance of *C. finmarchicus* (e.g. Heath et al., 2000; Speirs et al., 2004; Torgersen and Huse, 2005; Heath et al., 2008; Head et al., 2013; Melle et al., 2014). While some *C. finmarchicus* were caught deeper than 50 m in all basins, a very high proportion of the total *C. finmarchicus* population was concentrated in the upper 50 m (Fig. 7).

Abundance of *C. hyperboreus* in the MOCNESS data was highest in the Labrador Sea, with intermediate abundance in the Iceland Sea, and overall low levels in the Irminger and Norwegian Seas. In both the Iceland and Norwegian Seas the older stages dominated the population, whereas the smaller stages dominated in the western basins. This is reflected in the distribution of biomass of *C. hyperboreus* from the WP2 catches where *C. hyperboreus* was a major contributor to the biomass of the >2000 μm fraction in the Iceland Sea, while in the other areas the contribution was minimal. That *C. hyperboreus* is an important part of the larger copepod assembly in the Iceland Sea is further supported by the biomass estimated from abundance data (Fig. 14B). In the western areas, where the population was dominated by young stages of copepodites, the population was concentrated in the upper 50 m, whereas the older stages in the eastern areas distributed more evenly from the surface down to at least 200 m (Fig. 7). The Irminger Sea had the lowest *C. hyperboreus* biomass (Figs. 3 and 14B) which agrees with the findings of Gislason (2003).

Pseudocalanus spp. were common in the Norwegian and Iceland Seas and rare in the western basins while *Paraeuchaeta* spp. were most abundant in the Irminger Sea and least abundant in the Iceland Sea (Fig. 8). The females of *Pseudocalanus* were found down to several hundred meters in the Iceland Sea, but densities peaked near the surface. This is reflected in the distribution of the category "females with eggs" in the VPR (Fig. 13), which is suspected to be the adult females with egg sacs of *Pseudocalanus* spp. *Paraeuchaeta* spp. were the most deeply distributed copepod species that we looked more closely into. The *Paraeuchaeta* spp. are carnivorous species that feed on other copepods and perform extensive diel migrations into shallow waters during night (Yen, 1985; Fleddum et al., 2001; Skarra and Kaartvedt, 2003; Irigoien and Harris, 2006). These species also carry egg sacs, and may have contributed to the mentioned category of the VPR (see also Melle et al., this issue).

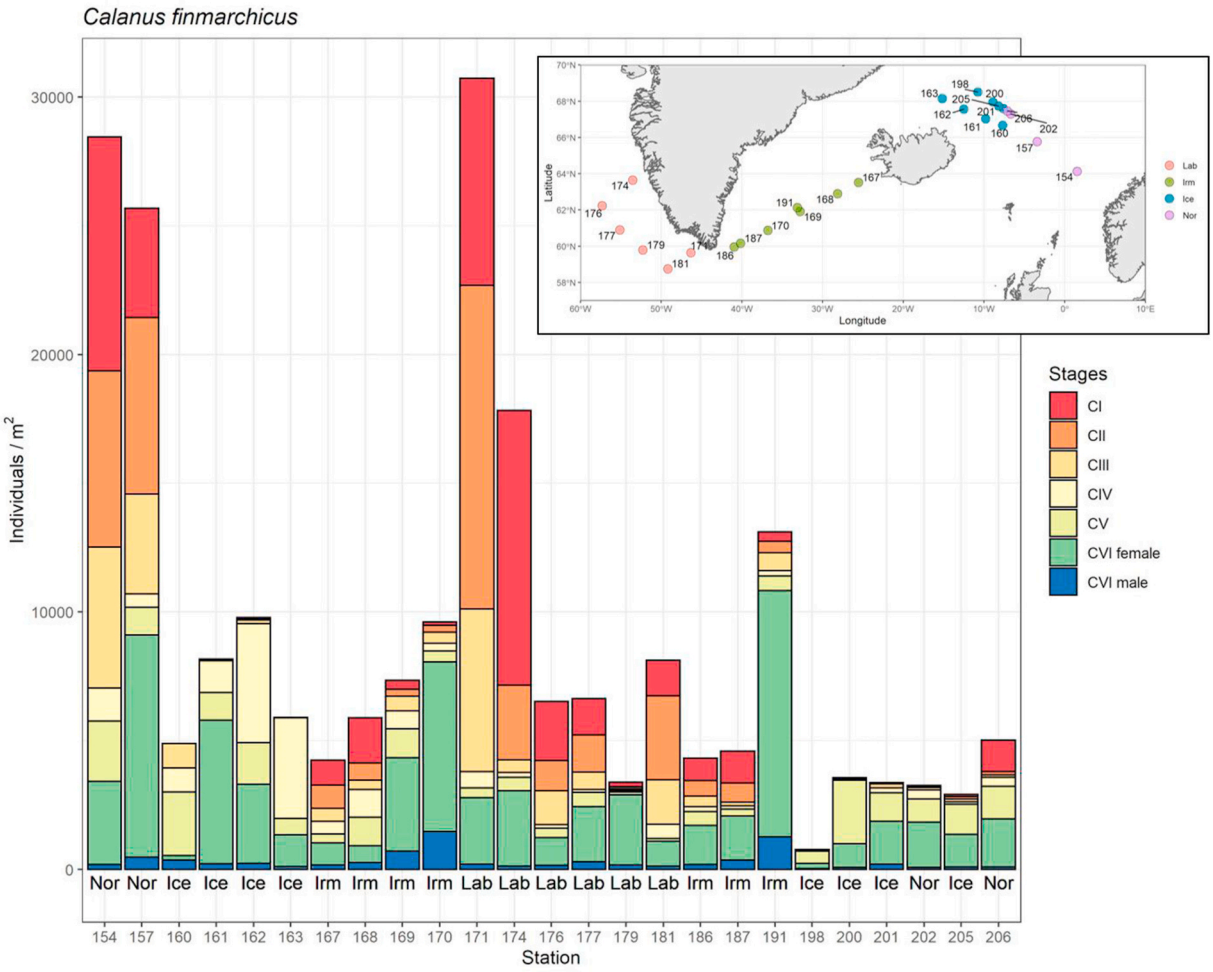

Fig. 9. Surface-integrated number of *Calanus finmarchicus* stages CI-CVI. From MOCNESS net samples (0–200 m). Along x-axis numbers denote station numbers and the abbreviations, Nor, Ice, Irm and Lab, denotes the four seas. The station to the left was the first station near Norway, the two first stations in the Labrador Sea were also visited during the westward survey, all stations after that are from the eastward survey.

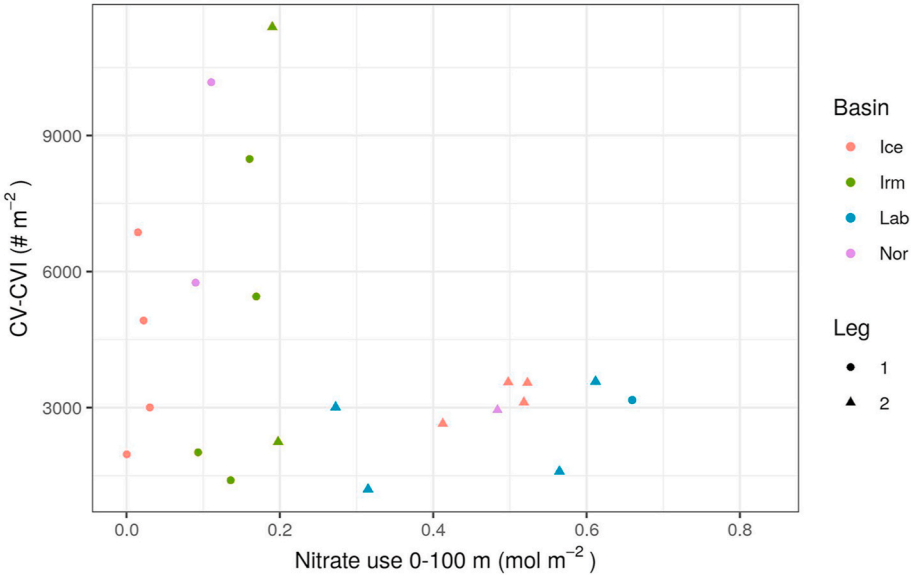

Fig. 10. Surface-integrated number of individuals of *Calanus finmarchicus* stages CV-CVI (# m^{-2}) from WP2 net samples (0–200 m) versus the depletion of nitrate (mol m^{-2}). See Naustvoll et al. (this issue).

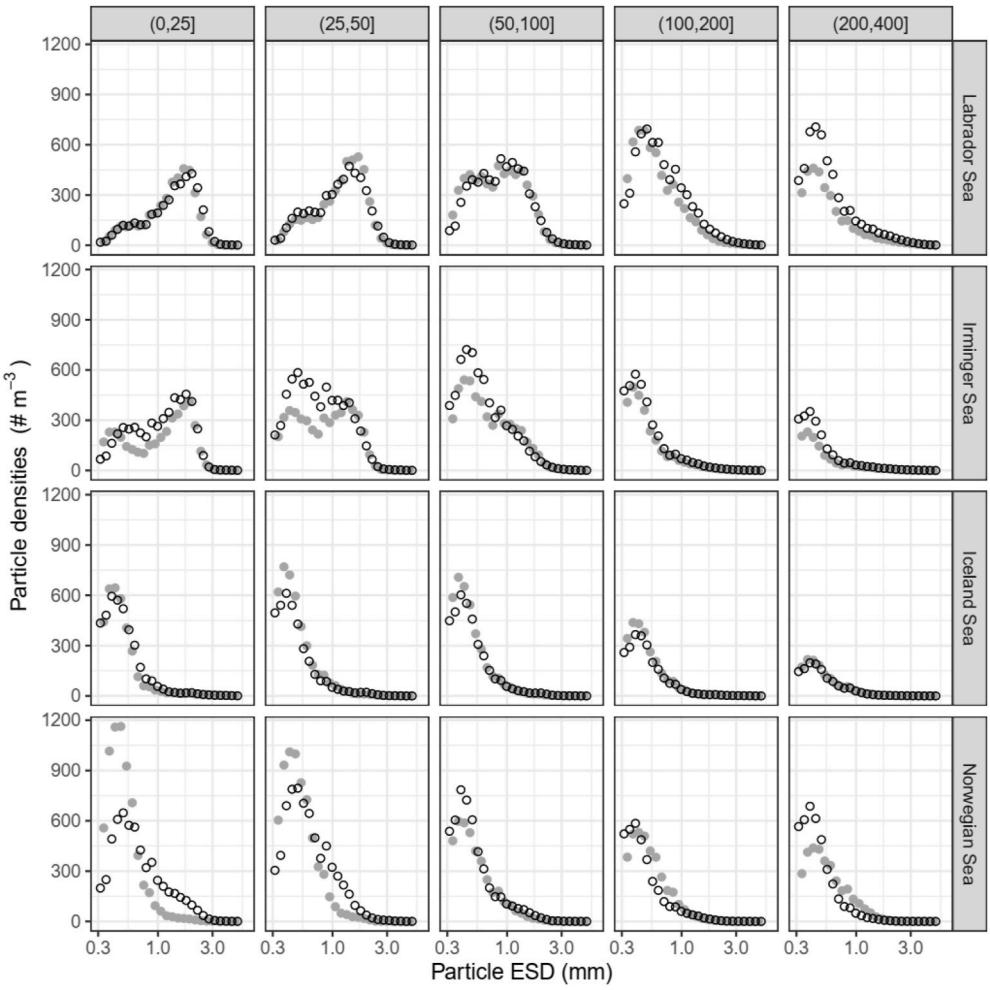

Fig. 11. OPC estimated densities of particles in different size-ranges, split according to depth and ocean area. Black circles show night-time data (solar elevation < 10), grey circles show daytime data.

4.2. Stage distribution and phenology of *Calanus finmarchicus*

Stage distribution of *C. finmarchicus* was interpreted as recruitment to G1 in the eastern Norwegian Sea and the West-Greenland Shelf of the Labrador Sea on the westward survey during the first half of May, as well in the Labrador Sea on the eastward survey during late May and early June. At weather Station Mike in the Norwegian Sea, number of CI peaked at more than 70 000 ind. m^{-2}, indicating that we did not see the peak of recruitment to G1 anywhere at the time of the cruise. The last station close to the Norwegian shelf was also dominated by G1. The other stations were dominated by G0. This interpretation is in line with the results reported for the Norwegian sea by Broms and Melle (2007), Broms et al. (2009) and Bagøien et al. (2012). They found that the phytoplankton bloom was delayed by 1 month from coastal to Arctic water masses in the Norwegian sea and recruitment to CI and CIII was delayed by 1–2 months. This fits with our interpretation that on the eastward leg, we still observed G0 close to the Arctic front (see also Melle et al., this issue) and mainly G1 near the Norwegian shelf in the east. Further west, in Arctic proper waters of the Iceland Sea, the recruitment to younger stages of the G1 peaked in June (Astthorsson and Gislason, 2003). Similarly, in the Labrador Sea, Head et al. (2013) showed that recruitment to G1 peaked in June–July, while the over-wintering generation diminished from May to July when it was reduced to low numbers. A similar pattern was observed on the Labrador shelf, while in the Eastern Labrador shelf the reproduction and subsequent recruitment to young copepodite stages of *C. finmarchicus* preceded the other two areas, as we also observed when entering the Labrador Sea on the westward survey, close to the Greenland Shelf.

Reproduction and stage development is dependent on both the onset of the spring bloom (Melle and Skjoldal, 1998; Niehoff et al., 1999; Hirche et al., 2001; Melle et al., 2014) as well as stage development being highly dependent on ambient temperature (Campbell et al., 2001; Kvile et al., 2014). Presence of young stages have thus been reported in post-bloom conditions in areas influenced by Arctic water (Broms et al., 2009; Plourde et al., 2009). In the Labrador Sea, a strong spring bloom was evident (Fig. 14), coinciding with young stages of G1 (Fig. 7). The young stages of *C. finmarchicus* in the Norwegian Sea would be subject to very different feeding conditions compared to the Labrador Sea (Fig. 14B), with the young stages present in the Norwegian Sea during the cruise evidently missing the spring bloom.

Broms and Melle (2007) states that "*When the number of individuals of each copepodite stage was plotted against the consumption of nitrate, representing the phytoplankton development, the same events in the life cycle of C. finmarchicus were found at similar nitrate consumptions in different geographical areas in the Norwegian Sea*". In Fig. 10, CV-CVI of the G0 were no longer present in the population at a nitrate use above 0.2–0.3 mol m^{-2}. This is at about the same level of depletion as reported by Broms and Melle (2007). Naustvoll et al., (this issue) showed that there was an inverse relationship between the shallowing depth of the mixed layer and the depletion of nitrate in the upper 100 m caused by algal growth. This shows that nitrate depletion can be used as a proxy for the development and timing of both the phytoplankton production and the

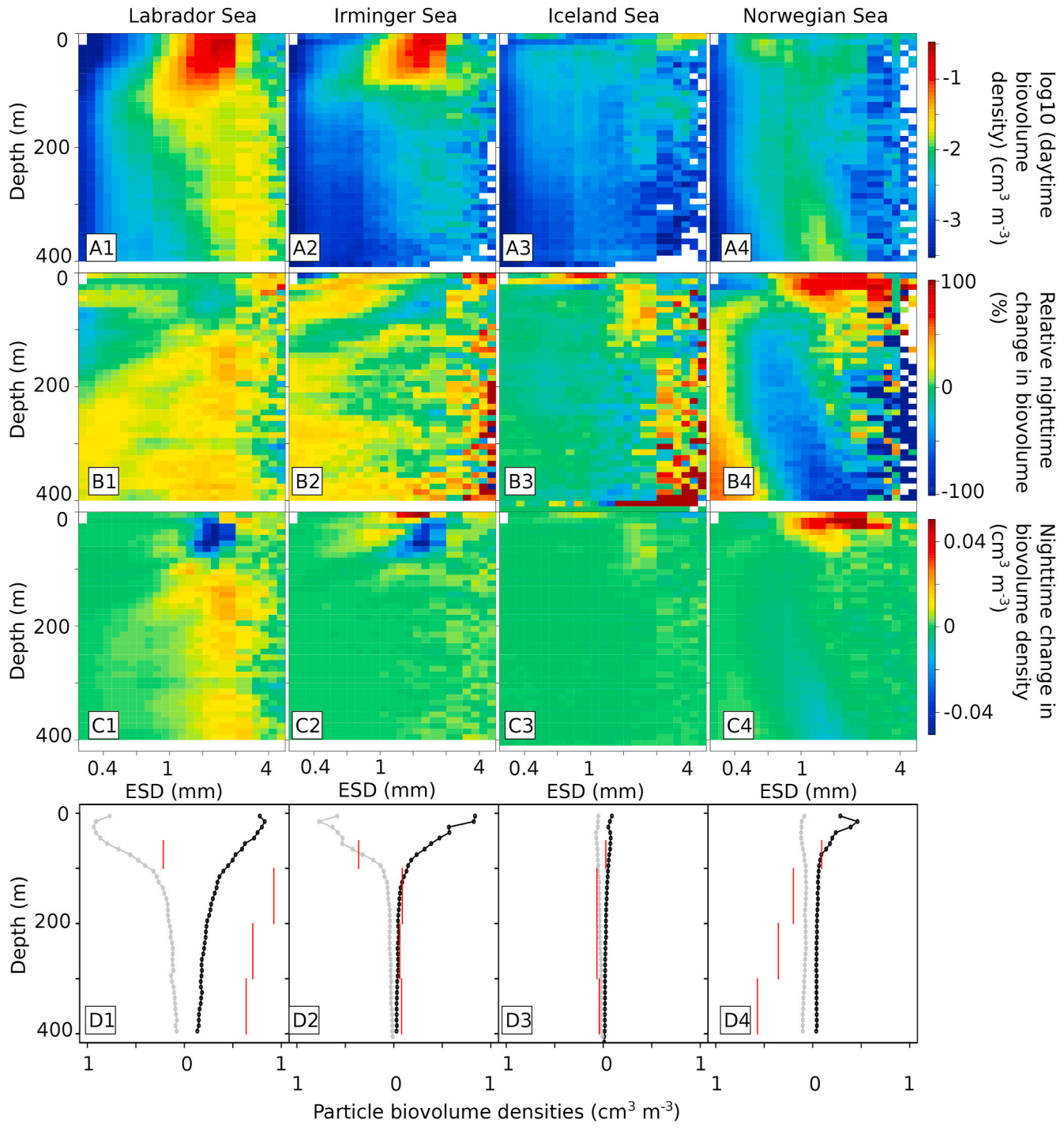

Fig. 12. A1-A4: OPC estimated daytime biovolume ($cm^3\ m^{-3}$) by particle equivalent spherical diameter (ESD, mm) and depth (m), for each of the 4 basins. B1–B4: day to night relative changes (%) in particle numbers by particle ESD and depth, with positive values signifying night-time increase. C1–C4: night to day difference in biovolume ($cm^3\ m^{-3}$) by size and depth, with positive values signifying night-time increase. D1-D4: biovolume distribution ($cm^3\ m^{-3}$) in the 0.5–2.5 mm ESD range, day (grey points and line) and night (black points and line). Red vertical bars show 1/10 of depth interval (vertical span) integrated night to day differences in particle biovolume ($cm^3\ m^{-2}$), with lines to the left of zero indicating net loss during night. Figures in the first column (A1-D1) are based on data from MESSOR deployments in the Labrador Sea, column 2 (A2-D2) are from Irminger Sea, column 3 (A3-D3) from Iceland Sea and A4-D4 from the Norwegian Sea. (For interpretation of the references to color in this figure legend, the reader is referred to the Web version of this article.)

population of *C. finmarchicus*. Further, it is an indication of the existence of a functional relationship leading from water column stabilisation, phytoplankton bloom development to development and reproduction of *C. finmarchicus* (Melle and Skjoldal, 1998; Broms and Melle, 2007; Bagøien et al., 2012). It has not previously been shown that this mechanism may be valid across water masses and basins.

4.3. Basin scale variation in abundance and biomass by optical methods

In all OPC density profiles, the density of particles smaller than ~0.4 mm ESD was low, suggesting that particles smaller than this were not sampled efficiently. Above a size of ~2.5 mm ESD variability in the measurements is very high, due to low overall counts, suggesting that

Table 4
Integrated OPC biovolume and estimated dry-weight of particles in the upper 0–200m for the three size fractions 0.5–1.0 mm, 1–2 mm, and 2–5 mm ESD day and night in the targeted basins. Vol2DW columns shows estimated dry-weights (biovol*0.2; Skjoldal et al., 2004) for the respective biovolumes.

Area	Time of Day	N casts	Biovolume 0–200 m (cm^3)			Vol2DW conversion (~g DW m^{-2})		
			Size fraction, ESD (mm)			Size fraction, ESD (mm)		
			0.5–1	1–2	2–5	0.5–1	1–2	2–5
Labrador Sea	Day	27	9.6	53.6	35.4	1.9	10.7	7.1
	Night	23	11.2	53.4	44.6	2.2	10.7	8.9
Irminger Sea	Day	16	5.3	31.2	18.3	1.1	6.2	3.7
	Night	21	6.8	29.2	17.9	1.4	5.9	3.6
Iceland Sea	Day	30	3.4	3.5	5.9	0.7	0.7	1.2
	Night	48	2.9	3.8	5.4	0.6	0.8	1.1
Norwegian Sea	Day	6	6.5	5.8	3.3	1.3	1.2	0.7
	Night	5	5.6	11.6	6.0	1.1	2.3	1.2

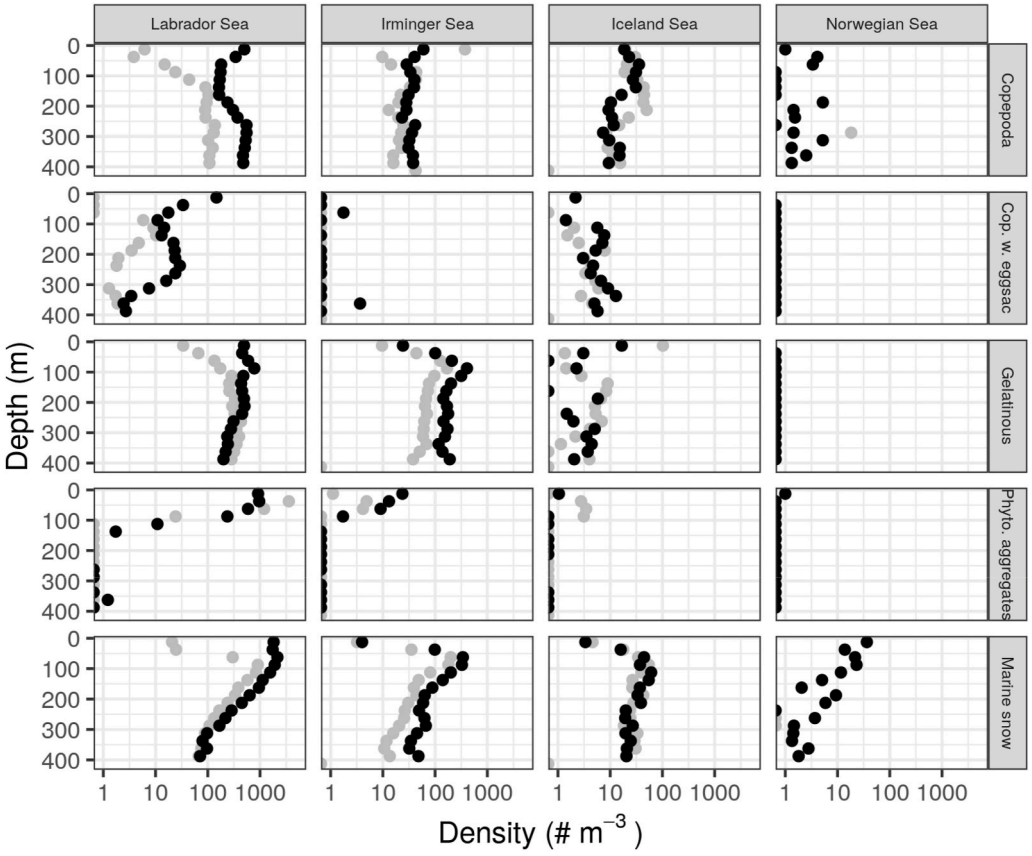

Fig. 13. Vertical profiles of densities of the identified categories from the VPR, split into day (grey points) and night (black points) and according to area.

larger particles are not efficiently measured, at least not at this aggregation level and unless the local densities were high (e.g. Labrador Sea). The highest average particle densities, even in the upper layers, were well below the upper limit of 10^4 m^{-3} previously suggested as an upper limit for the OPC (Herman et al., 2004). These high particle concentrations were estimated in the Norwegian Sea, however the average size of these particles were small. The distributions of particle densities measured by the OPC may suggest that coincidence counts were a problem at shallow depths in the western basins (Fig. 11), since particle size distributions peaked at intermediate size, with very few small particles registered, coinciding with peaks in the sum of particle cross-sections. However, these peaks in the biovolume spectra also coincide with the location of peaks predicted from the copepods in the MOCNESS catches (Fig. 14), which may suggest that they are not an artefact.

Even at greater depths in the Labrador and Irminger Sea, where particle concentrations presumably were low enough to allow proper quantification of particle spectra by the OPC, the concentration of larger particles were higher than in the eastern basins. Also, if coincidence counts were a major influence on the surface near observations in the western basins, it is unclear why the night-time density reductions (Fig. 12 B1–B4) were restricted to a relatively narrow size-range. The VPR data suggested that the concentrations of all identified components (e.g. copepods, gelatinous plankton and marine snow) were higher in the western basins, which contrasts with observations from MOCNESS data.

The plots of OPC biovolume densities (Fig. 12 A1-A4) showed that the particle sizes are shifted towards larger sizes in the western basins, even at depth. We assume that this shift reflects actual size-differences, although the OPC estimates particle sizes based on light attenuation, and particle transparency may therefore have an effect (Herman, 1992). Larger particles, all other factors being equal, have a higher probability

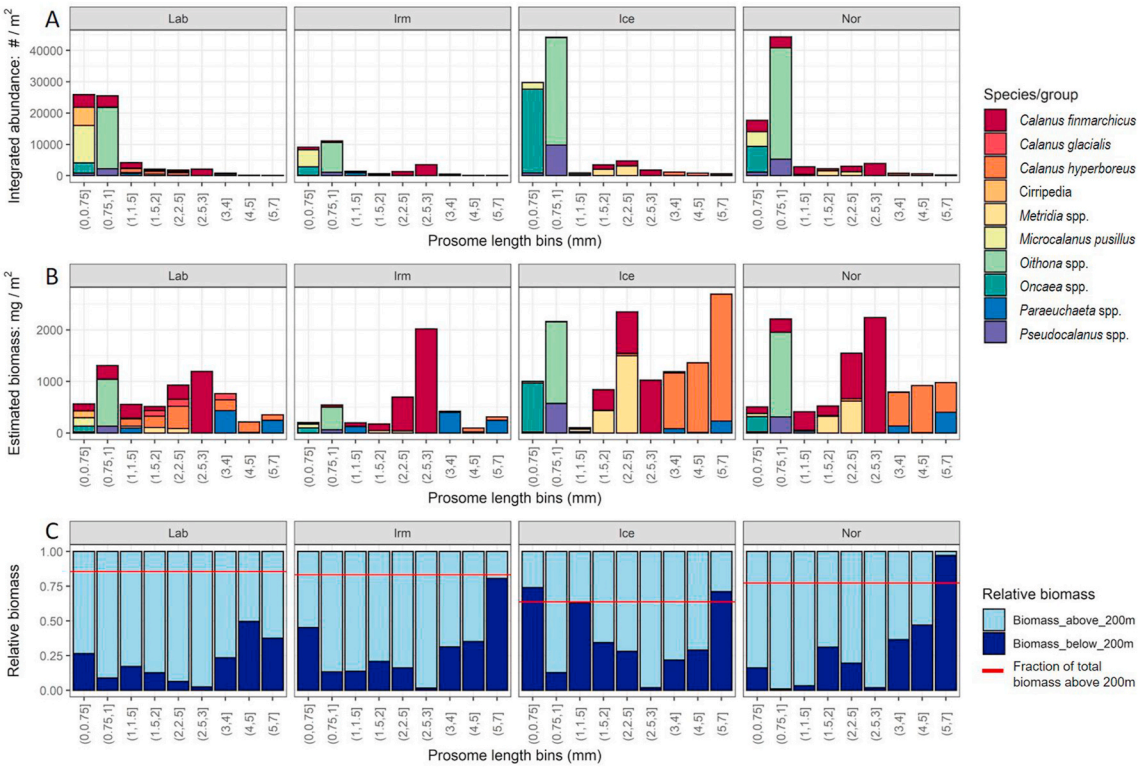

Fig. 14. Abundance and biomass by prosome length groups. Row A shows the integrated abundance (0–1000m) of common mesozooplankton divided into prosome length groups from MOCNESS samples. Row B shows the calculated biomass given prosome lengths (Peters, 1983). Row C bars shows the relative abundance of biomass above and below 200m, while the red line shows the fraction of total biomass in each basin positioned above 200m. (For interpretation of the references to color in this figure legend, the reader is referred to the Web version of this article.)

of being identified in the VPR data (e.g. more pixels available), relative biases are therefore possible in the profiles of identified plankton. In the Iceland Sea, where the abundance was dominated by small species (*Oithona* spp., *Oncaea* spp.) in the upper waters, the VPR estimated total copepod densities at least one order of magnitude below the MOCNESS estimates (Fig. 6). On the other hand, in the Labrador Sea, where large calanoid copepods made up more than 50% of the total mesozooplankton abundance in the upper 50 m, VPR and MOCNESS estimates are of the same order of magnitude, down to a depth of 200 m. Below 200 m, however, the VPR estimates are at least 1 order of magnitude higher. The ratios of copepods to total identified particles in the VPR data were very low in the 50–200 m depth range in the Labrador Sea (not shown). This is a result of high densities of both algal aggregates and marine snow in this depth range (Fig. 13), as densities of copepods for this depth range in the Labrador Sea generally exceeded those registered in the other areas.

In the Labrador Sea the VPR registered high densities of marine snow (Fig. 13) in addition to high densities of phytoplankton in the upper waters. Densities of (large) marine snow particles seen in the VPR data were also relatively high (e.g. ~100 m^{-3}) down towards 400 m depth. In the Labrador Sea the sensors on both the CTD and the towed body also registered relatively high fluorescence signals all the way down to 400 m (Fig. 15). The high fluorescence values were detected at depth both night and day, documenting that in this area vertical flux from the upper layer was intense. Similar patterns have been previously found during spring bloom in the North Atlantic (Briggs et al., 2011). This vertical flux of particles with still active chlorophyll could potentially also serve as a source of food for the mesozooplankton at depth (Moller et al., 2012), and is one potential factor in explaining why densities of copepods observed with the VPR increased with depth in the Labrador Sea.

4.4. Day night differences in particle/species vertical distribution

In the Norwegian Sea, the concentration of particles in the range from ~1 to 2.5 mm ESD (the size range expected to be most effectively sampled by the OPC) from ~100 m and downwards was lower during the night, and a corresponding increase in surface-near densities was observed (Fig. 12 B4). Despite few casts, this corresponds to the classic pattern of DVM. The same pattern of reduction in the 1–2.5 mm class at depth was detectable also in the Iceland Sea (Fig. 12 B3), although clearly weaker. Especially in the Norwegian Sea data there is an indication that biovolume loss during night occurs from progressively larger size-classes as depth increases (Fig. 12 B4, C4), indicating that there is a correlation between organism size and migration amplitude. Diel changes in biovolume in the western areas were different, with a clear reduction in biovolume densities in the near-surface waters (down to 80 m) during the night, apart from in the very shallowest measured depth range in the Irminger Sea (Fig. 12 C1–C2).

A potential explanation for the observed diel changes in biovolume would be a diel signal in the vertical distribution of algal aggregates (bloom category in the VPR data) and marine snow. Previous studies have shown that densities of marine snow can vary over the diel cycle (e.g. Lampitt et al., 1993). The near-surface reduction co-occurred with an increase in particle densities at depth during night (Fig. 12 C1), and the overall diel pattern in biovolume changes were similar for both the Labrador and Irminger Sea, despite the differences in the overall particle (Fig. 11) and marine snow densities (Fig. 13) in these two areas. In the Labrador Sea, in particular, a relatively high proportion of particles identified at depth with the VPR (Fig. 13) were copepods, and densities of copepods in deep waters were higher (Labrador Sea) or similar (Irminger Sea) during night, suggesting that the pattern observed in the OPC data is influenced by diel patterns in copepod densities. The observed pattern of night-time reduction in biovolume near the surface

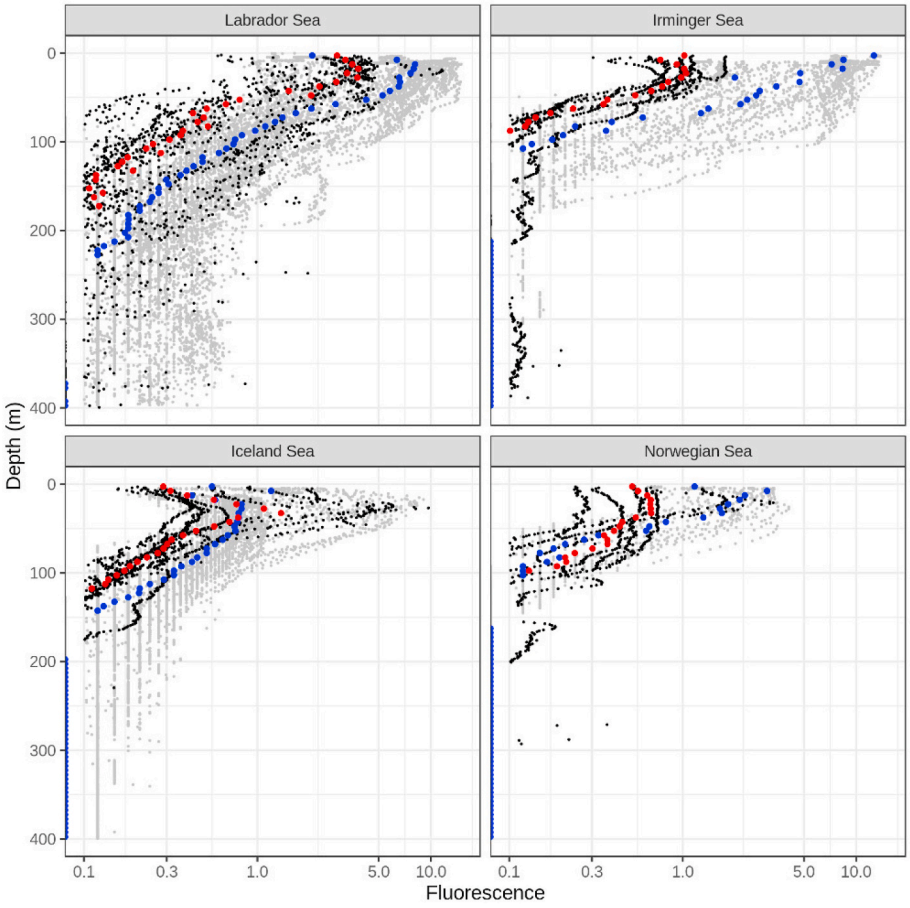

Fig. 15. Fluorescence data from the tow-body (grey points show 5 s averages for all deployments), and from vertical SeaBird 911plus CTD casts (black points are averages for 5 m bins from stations with MOCNESS deployments). Blue points show vertical averages for 5 m bins over all MESSOR deployments, red points are vertical averages for 5 m bins over all Seabird 911plus CTD deployments. (For interpretation of the references to color in this figure legend, the reader is referred to the Web version of this article.)

is compatible with reverse diel vertical migration, and the overall patterns of diel biovolume change (Fig. 12 C1–C2) were similar in both the Labrador and Irminger Seas.

Traditionally "normal" DVM, where the organisms swim toward the productive surface waters under the cover of darkness, is seen as an adaptation to minimize the impacts of visual predation (Hays, 2003). Conversely, reverse DVM has usually been explained as an adaptation to cope with a dielly migrating predator (Ohman et al., 1983). The eastern areas had epipelagic fish present during daytime (Klevjer et al., this issue a, b; Melle et al., this issue), whereas backscatter from epipelagic schooling fish were largely absent in the western areas (Klevjer et al., this issue b), suggesting that for mesozooplankton, average predator fields in the epipelagic during daytime differed between the areas. In both areas DVM of mesopelagic nekton was observed, giving rise to increased densities of planktivorous nekton in upper waters during the night. The densities of gelatinous organisms observed with the VPR were high in the western basins (see also Klevjer et al., this issue a), and at least for the Labrador Sea the VPR data suggests that this group performed normal DVM (Fig. 11). Of the 2 groups of Schypozoans dominating the trawl catches in the western areas (*Atolla* sp., *Periphylla periphylla*, Klevjer et al., this issue a, b), at least one is known to be a vertically migrating species (e.g. Kaartvedt et al., 2011). Dielly migrating predatory gelatinous plankton normally do not rely on vision to capture prey and would have increased the predation pressure on mesozooplankton in the epipelagic during night especially in the western areas, since biomasses were higher here. In sum the data suggest that in the western areas there would have been increased predation pressure on the mesozooplankton size-fraction in the epipelagic during night, since densities of both visual and non-visual planktivores were low in the epipelagic during day. This increased nocturnal predation pressure could presumably be a "driving force" behind the observed reverse DVM of mesozooplankton in these areas.

4.5. *Strengths, weaknesses and variation in sampling gear*

The data from our cruise span different phases of the spring bloom in the different basins, with fluorescence levels indicating that the bloom was ongoing in the Labrador Sea, and that we were in pre-bloom conditions in the Irminger Sea and later or post-bloom conditions in the Norwegian Sea during the return (see Naustvoll et al., this issue). As such, the results obtained only provide a snapshot of the local conditions during our passing. In the Labrador Sea, delaying the cruise by just one week would presumably have significantly increased the biomass of *C. finmarchicus*, as chlorophyll levels were high, and the population here was dominated by early copepodite stages. Data obtained from identification and enumeration of net catches are necessary to understand taxonomic composition as well as population dynamics and state. From the composition of the net catches it was found that the abundance of small copepods in the upper 25m were almost one order of magnitude higher in the eastern basins, especially in the Norwegian Sea. While this could be a temporal pattern related to the timing of the cruise in relation to the phenology of the zooplankton community, it does suggest that at the time of the cruise, the overall ecology in the upper 25 m were very different from east to west.

Since nets are labour intensive to work up, it is hard to obtain enough data to study all aspects of plankton ecology in a robust and meaningful way. Using just the net-samples from the cruise, it would for instance be difficult to evaluate DVM patterns for the 4 basins. The OPC data shows that day and night differences in particle distributions differs between the eastern and western basins, with classical DVM (e.g. deep during the day, shallow during the night) indicated for larger mesozooplankton in the eastern basins, and reverse DVM in the western. This pattern could

be related to the relative timing of sampling in relation to the bloom, to latitudinal differences (generally the sampling in the eastern basins were further north), to differences in the primary production or to the predator field (more gelatinous plankton in the western basins, more epipelagic (Melle et al., this issue) and possibly migrating mesopelagic (Klevjer et al., this issue a, b) fish in the eastern basins). However, it could also be related to other ecological or environmental factors such as phytoplankton aggregates formation and increased chlorophyll levels at depth in the Labrador Sea as discussed above, and the high resolution of OPC data allows us to identify such patterns. Given the relatively small observation volume of the VPR, small errors in the estimated observation volume of the VPR can give rise to large errors in the estimated densities (Basedow et al., 2013). With an observation volume of ~150 mL per image, relatively high abundances are also needed to give accurate density estimates, at an average density of 100 copepods per m^3 one would only expect one observation per ~4 s at 15 Hz frame rate. In our case the VPR seems to have a too small sampling volume to identify the patterns seen in the OPC data, but it allows us to identify the particles seen by the OPC, and gives us information on gelatinous organisms, marine snow and phytoplankton aggregates, which otherwise can be difficult to sample properly. These categories dominated the VPR objects that we could identify (Melle et al., this issue).

CRediT authorship contribution statement

Espen Strand: Conceptualization, Formal analysis, Investigation, Writing - original draft, Visualization. **Thor Klevjer:** Conceptualization, Formal analysis, Investigation, Writing - original draft, Visualization. **Tor Knutsen:** Investigation, Writing - review & editing. **Webjørn Melle:** Conceptualization, Investigation, Writing - review & editing, Project administration, Funding acquisition.

Declaration of competing interest

The authors declare that they have no known competing financial interests or personal relationships that could have appeared to influence the work reported in this paper.

Acknowledgement

We would like to thank the captain and crew of R/V G. O. Sars for their skilled operations during our cruise from Bergen to Nuuk during May and June 2013. The sampling, data analysis and reporting have been supported by IMR through funding of shiptime, laboratory costs and salaries of researchers through internally funded projects. We would like to extend our gratitude to two anonymous reviewers who helped improve the manuscript significantly. We would also like to acknowledge the funding from Euro-BASIN, EU FP7, Grant agreement No 264933, HARMES, Research Council of Norway project number 280546 and MEESO, EU H2020 research and innovation programme, Grant Agreement No 817669.

References

Aksnes, D.L., Blindheim, J., 1996. Circulation patterns in the North Atlantic and possible impact on population dynamics of *Calanus finmarchicus*. Ophelia 44, 7–28. https://doi.org/10.1080/00785326.1995.10429836.

Astthorsson, O.S., Gislason, A., 2003. Seasonal variations in abundance, development and vertical distribution of *Calanus finmarchicus, C. hyperboreus* and *C. glacialis* in the East Icelandic Current. J. Plankton Res. 25, 843–854.

Bagøien, E., Melle, W., Kaartvedt, S., 2012. Seasonal development of mixed layer depths, nutrients, chlorophyll and *Calanus finmarchicus* in the Norwegian Sea - a basin-scale habitat comparison. Prog. Oceanogr. 103, 58–79. https://doi.org/10.1016/j.pocean.2012.04.014.

Basedow, S.L., Tande, K.S., Norrbin, M.F., Kristiansen, S.A., 2013. Capturing quantitative zooplankton information in the sea: performance test of laser optical plankton counter and video plankton recorder in a *Calanus finmarchicus* dominated summer situation. Prog. Oceanogr. 108, 72–80. https://doi.org/10.1016/j.pocean.2012.10.005.

Blindheim, J., 2004. Oceanography and climate. In: Skjoldal, H.R. (Ed.), The Norwegian Sea Ecosystem. Tapir Academic Press, Trondheim, pp. 65–96.

Briggs, N., Perry, M.J., Cetinic, I., Lee, C., D'Asaro, E., Gray, A.M., Rehm, E., 2011. High-resolution observations of aggregate flux during a sub-polar North Atlantic spring bloom. Deep-Sea Res. Part I-Oceanogr. Res. Pap. 58, 1031–1039. https://doi.org/10.1016/j.dsr.2011.07.007.

Broms, C., Melle, W., 2007. Seasonal development of *Calanus finmarchicus* in relation to phytoplankton bloom dynamics in the Norwegian Sea. Deep Sea Res. Part II Top. Stud. Oceanogr. 54, 2760–2775.

Broms, C., Melle, W., Kaartvedt, S., 2009. Oceanic distribution and life cycle of *Calanus* species in the Norwegian Sea and adjacent waters. Deep Sea Res. Part II Top. Stud. Oceanogr. 56, 1910–1921. https://doi.org/10.1016/j.dsr2.2008.11.005.

Bucklin, A., Kaartvedt, S., Guarnieri, M., Goswami, U., 2000. Population genetics of drifting (*Calanus* spp.) and resident (*Acartia clausi*) plankton in Norwegian fjords. J. Plankton Res. 22 (7), 1237–1251. https://doi.org/10.1093/plankt/22.7.1237.

Campbell, R.G., Wagner, M.M., Teegarden, G.J., Boudreau, C.A., Durbin, E.G., 2001. Growth and development rates of the copepod *Calanus finmarchicus* reared in the laboratory. Mar. Ecol. Prog. Ser. 221, 161–183.

Castellani, C., Irigoien, X., Harris, R.P., Holliday, N.P., 2007. Regional and temporal variation of *Oithona spp*. biomass, stage structure and productivity in the Irminger Sea, North Atlantic. J. Plankton Res. 29, 1051–1070. https://doi.org/10.1093/plankt/fbm079.

Chiba, S., Batten, S.D., Yoshiki, T., Sasaki, Y., Sasaoka, K., Sugisaki, H., Ichikawa, T., 2015. Temperature and zooplankton size structure: climate control and basin-scale comparison in the North Pacific. Ecol. Evol. 5, 968–978. https://doi.org/10.1002/ece3.1408.

Choquet, M., Kosobokova, K., Kwaśniewski, S., Hatlebakk, M., Dhanasiri, A.K.S., Melle, W., Daase, M., Svensen, C., Søreide, J.E., Hoarau, G., 2018. Can morphology reliably distinguish between the copepods *Calanus finmarchicus* and *C. glacialis*, or is DNA the only way? Limnol Oceanogr. Methods 16, 237–252.

Conover, R.J., 1988. Comparative life histories in the genera *Calanus* and *Neocalanus* in high-latitudes of the northern hemisphere. Hydrobiologia 167, 127–142. https://doi.org/10.1007/bf00026299.

Conway, D., 2006. Identification of the Copepodite Developmental Stages of Twenty-Six North Atlantic Copepods. Occasional Publications. Marine Biological Association of the United Kingdom, No. 2, Plymouth, United Kingdom, p. 28p.

Davis, C.S., Gallager, S.M., Berman, M.S., Haury, L.R., Strickler, J.R., 1992. The video plankton recorder (VPR): design and initial results. Archiv fuer Hydrobiologie, Beiheft: Ergeb. Limnol. 36, 67–81.

Davis, C.S., Thwaites, F.T., Gallager, S.M., Hu, Q., 2005. A three-axis fast-tow digital Video Plankton Recorder for rapid surveys of plankton taxa and hydrography. Limnol Oceanogr. Methods 3, 59–74. https://doi.org/10.4319/lom.2005.3.59.

Drinkwater, K. F., Sundby, S., Wiebe, P. this issue. Exploring the hydrography of the boreal/arctic domains of North Atlantic seas: results from the 2013 BASIN survey. Deep-Sea Res. II.

Durbin, E., Kane, J., 2007. Seasonal and spatial dynamics of Centropages typicus and C. hamatus in the western North Atlantic. Prog. Oceanogr. 72, 249–258.

Falk-Petersen, S., Mayzaud, P., Kattner, G., Sargent, J., 2009. Lipids and life strategy of Arctic *Calanus*. Mar. Biol. Res. 5, 18–39. https://doi.org/10.1080/17451000802512267.

Fleddum, A., Kaartvedt, S., Ellertsen, B., 2001. Distribution and feeding of the carnivorous copepod Paraeuchaeta norvegica in habitats of shallow prey assemblages and midnight sun. Mar. Biol. 139, 719–726.

Fraser, J.H., 1966. Zooplankton sampling. Nature 221, 915–916.

Gabrielsen, T.M., Merkel, B., Søreide, J.E., Johansson-Karlsson, E., Bailey, A., Vogedes, D., Nygård, H., Varpe, Ø., Berge, J., 2012. Potential misidentifications of two climate indicator species of the marine arctic ecosystem: *Calanus glacialis* and *C. finmarchicus*. Polar Biol. 35, 1621–1628.

Gallienne, C.P., Robins, D.B., 2001. Is *Oithona* the most important copepod in the world's oceans? J. Plankton Res. 23, 1421–1432. https://doi.org/10.1093/plankt/23.12.1421.

Gislason, A., 2003. Life-cycle strategies and seasonal migrations of oceanic copepods in the Irminger Sea. Hydrobiologia 503, 195–209. https://doi.org/10.1023/B:HYDR.0000008498.87941.7d.

Gislason, A., Silva, T., 2012. Abundance, composition, and development of zooplankton in the Subarctic Iceland Sea in 2006, 2007, and 2008. ICES J. Mar. Sci. 69, 1263–1276. https://doi.org/10.1093/icesjms/fss070.

Hays, G.C., 2003. A review of the adaptive significance and ecosystem consequences of zooplankton diel vertical migrations. Hydrobiologia 503, 163–170. https://doi.org/10.1023/B:HYDR.0000008476.23617.b0.

Head, E.J.H., Harris, L.R., Yashayaev, I., 2003. Distributions of *Calanus* spp. and other mesozooplankton in the Labrador Sea in relation to hydrography in spring and summer (1995-2000). Prog. Oceanogr. 59, 1–30. https://doi.org/10.1016/s0079-6611(03)00111-3.

Head, E.J.H., Melle, W., Pepin, P., Bagøien, E., Broms, C., 2013. On the ecology of *Calanus finmarchicus* in the subarctic north Atlantic: a comparison of population dynamics and environmental conditions in areas of the Labrador Sea-Labrador/Newfoundland shelf and Norwegian sea Atlantic and coastal waters. Prog. Oceanogr. 114, 46–63. https://doi.org/10.1016/j.pocean.2013.05.004.

Heath, M.R., Fraser, J.G., Gislason, A., Hay, S.J., Jonasdottir, S.H., Richardson, K., 2000. Winter distribution of *Calanus finmarchicus* in the northeast Atlantic. ICES J. Mar. Sci. 57, 1628–1635. https://doi.org/10.1006/jmsc.2000.0978.

Heath, M.R., Boyle, P.R., Gislason, A., Gurney, W.S.C., Hay, S.J., Head, E.J.H., Holmes, S., Ingvarsdottir, A., Jonasdottir, S.H., Lindeque, P., Pollard, R.T., Rasmussen, J., Richards, K., Richardson, K., Smerdon, G., Speirs, D., 2004. Comparative ecology of over-wintering *Calanus finmarchicus* in the northern North

Atlantic, and implications for life-cycle patterns. ICES J. Mar. Sci. 61, 698–708. https://doi.org/10.1016/j.icesjms.2004.03.013.

Heath, M.R., Rasmussen, J., Ahmed, Y., Allen, J., Anderson, C.I.H., Brierley, A.S., Brown, L., Bunker, A., Cook, K., Davidson, R., Fielding, S., Gurney, W.S.C., Harris, R., Hay, S., Henson, S., Hirst, A.G., Holliday, N.P., Ingvarsdottir, A., Irigoien, X., Lindeque, P., Mayor, D.J., Montagnes, D., Moffat, C., Pollard, R., Richards, S., Saunders, R.A., Sidey, J., Smerdon, G., Speirs, D., Walsham, P., Waniek, J., Webster, L., Wilson, D., 2008. Spatial demography of *Calanus finmarchicus* in the Irminger Sea. Prog. Oceanogr. 76, 39–88. https://doi.org/10.1016/j.pocean.2007.10.001.

Herman, A.W., 1992. Design and calibration of a new optical plankton counter capable of sizing small zooplankton. Deep Sea Res. Part A. Oceanographic Research Papers 39, 395–415. https://doi.org/10.1016/0198-0149(92)90080-D.

Herman, A.W., Beanlands, B., Phillips, E.F., 2004. The next generation of optical plankton counter: the laser-OPC. J. Plankton Res. 26, 1135–1145. https://doi.org/10.1093/plankt/fbh095.

Hirche, H.-J., Brey, T., Niehoff, B., 2001. A high-frequency time series at ocean Weather ship station M (Norwegian Sea): population dynamics of *Calanus finmarchicus*. Mar. Ecol.: Prog. Ser. 219, 205–219. https://doi.org/10.3354/meps219205.

Holliday, N.P., Waniek, J.J., Davidson, R., Wilson, D., Brown, L., Sanders, R., Pollard, R. T., Allen, J.T., 2006. Large-scale physical controls on phytoplankton growth in the Irminger Sea Part I: hydrographic zones, mixing and stratification. J. Mar. Syst. 59, 201–218. https://doi.org/10.1016/j.jmarsys.2005.10.004.

Irigoien, X., Harris, R.P., 2006. Comparative population structure, abundance and vertical distribution of six copepod species in the North Atlantic: evidence for intraguild predation? Mar. Biol. Res. 2, 276–290. https://doi.org/10.1080/17451000600865321.

Kaartvedt, S., Titelman, J., Rostad, A., Klevjer, T.A., 2011. Beyond the average: diverse individual migration patterns in a population of mesopelagic jellyfish. Limnol. Oceanogr. 56, 2189–2199. https://doi.org/10.4319/lo.2011.56.6.2189.

Klevjer, T.A., Melle, W., Knutsen, T., Aksnes, D.L., this issue b. Vertical distribution and migration of mesopelagic scatterers in four north Atlantic basins. Deep-Sea Res. Part II.

Klevjer, T., Melle, W., Knutsen, T., Strand, E., Korneliussen, R., Dupont, N., Salvanes, A. G.V., Wiebe, P.H., this issue a. Micronekton biomass distribution, improved estimates across four north Atlantic basins. Deep Sea Res. Part Top. Stud. Oceanogr., 104691.https://doi.org/10.1016/j.dsr2.2019.104691.

Knutsen, T., Melle, W., Mjanger, M., Strand, E., Fuglestad, A.L., Broms, C., Bagøien, E., Fitje, H., Ørjansen, O., Vedeler, T., 2013. MESSOR - A Towed Underwater Vehicle for Quantifying and Describing the Distribution of Pelagic Organisms and Their Physical Environment. OCEANS - Bergen, 2013 MTS/IEEE, pp. 1–12. https://doi.org/10.1109/OCEANS-Bergen.2013.6608177.

Knutsen, T., Wiebe, P.H., Gjøsæter, H., Ingvaldsen, R.B., Lien, G., 2017. High latitude epipelagic and mesopelagic scattering layers - a reference for future arctic ecosystem change. Front. Mar. Sci. 4, 334. https://doi.org/10.3389/fmars.2017.00334.

Kulagin, D.N., Neretina, T.V., 2017. Genetic and morphological diversity of the cosmopolitan chaetognath *Pseudosagitta maxima* (Conant, 1896) in the Atlantic Ocean and its relationship with the congeneric species. ICES J. Mar. Sci. 74, 1875–1884. https://doi.org/10.1093/icesjms/fsw255.

Kvile, K.O., Dalpadado, P., Orlova, E., Stenseth, N.C., Stige, L.C., 2014. Temperature effects on *Calanus finmarchicus* vary in space, time and between developmental stages. Mar. Ecol. Prog. Ser. 517, 85–104. https://doi.org/10.3354/meps11024.

Lampitt, R.S., Hillier, W.R., Challenor, P.G., 1993. Seasonal and diel variation in the open ocean concentrations of marine snow aggregates. Nature 362, 737–739. https://doi.org/10.1038/362737a0.

Lindeque, P.K., Hay, S.J., Heath, M.R., Ingvarsdottir, A., Rasmussen, J., Smerdon, G.R., Waniek, J.J., 2006. Integrating conventional microscopy and molecular analysis to analyse the abundance and distribution of four *Calanus* congeners in the North Atlantic. J. Plankton Res. 28, 221–238.

Madsen, S.D., Nielsen, T., Hansen, B.W., 2001. Annual population development and production by *Calanus finmarchicus, C. glacialis* and *C. hyperboreus* in Disko Bay, western Greenland. Mar. Biol. 139, 75–93. https://doi.org/10.1007/s002270100552.

Martin, E.S., Harris, R.P., Irigoien, X., 2006. Latitudinal variation in plankton size spectra in the Atlantic Ocean. Deep Sea Res. Part II Top. Stud. Oceanogr. 53, 1560–1572. https://doi.org/10.1016/j.dsr2.2006.05.006.

McLaren, I.A., Sevigny, J.M., Corkett, C.J., 1988. Body sizes, development rates, and genome sizes among *Calanus* species. Hydrobiologia 167, 275–284. https://doi.org/10.1007/BF00026315.

Melle, W., Skjoldal, H.R., 1998. Reproduction and development of *Calanus finmarchicus, C. glacialis* and *C. hyperboreus* in the Barents sea. Mar. Ecol. Prog. Ser. 169, 211–228. https://doi.org/10.3354/meps169211.

Melle, W., Klevjer, T.A., Strand, E., Slotte, A., Huse, G., this issue. Fine scale observations of the herring feeding migration at the Arctic front. Deep-Sea Research Part II: Topical Studies in Oceanography.

Melle, W., Ellertsen, B., Skjoldal, H.R., 2004. Zooplankton: the link to higher trophic levels. In: Skjoldal, H.R. (Ed.), The Norwegian Sea Ecosystem. Tapir Academic Press, Trondheim, pp. 137–202.

Melle, W., Runge, J., Head, E., Plourde, S., Castellani, C., Licandro, P., Pierson, J., Jonasdottir, S., Johnson, C., Broms, C., Debes, H., Falkenhaug, T., Gaard, E., Gislason, A., Heath, M., Niehoff, B., Nielsen, T.G., Pepin, P., Stenevik, E.K., Chust, G., 2014. The North Atlantic Ocean as habitat for *Calanus finmarchicus*: environmental factors and life history traits. Prog. Oceanogr. 129, 244–284. https://doi.org/10.1016/j.pocean.2014.04.026.

Moller, K.O., St John, M., Temming, A., Floeter, J., Sell, A.F., Herrmann, J.P., Mollmann, C., 2012. Marine snow, zooplankton and thin layers: indications of a trophic link from small-scale sampling with the Video Plankton Recorder. Mar. Ecol. Prog. Ser. 468, 57–69. https://doi.org/10.3354/meps09984.

Motoda, S., 1959. Devices of simple plankton apparatus. Mem. Fac. Fish. Hokkaido Univ. 7, 73–94.

Naustvoll, L., Melle, W., Klevjer, T.A., Drinkwater, K.F., Strand, E., Knutsen, T., This Issue. Dynamics of Primary Production and Species Diversity of Phytoplankton in the North Atlantic during Spring and Summer - a Trans-Atlantic Survey.

Niehoff, B., Klenke, U., Hirche, H.J., Irigoien, X., Head, R., Harris, R., 1999. A high frequency time series at Weathership M, Norwegian Sea, during the 1997 spring bloom: the reproductive biology of *Calanus finmarchicus*. Mar. Ecol. Prog. Ser. 176, 81–92. https://doi.org/10.3354/meps176081.

Nielsen, T., Kjellerup, S., Smolina, I., Hoarau, G., Lindeque, P., 2014. Live discrimination of *Calanus glacialis* and *C. finmarchicus* females: can we trust phenological differences? Mar. Biol. 161, 1299–1306. https://doi.org/10.1007/s00227-014-2419-5.

Ohman, M.D., Frost, B.W., Cohen, E.B., 1983. Reverse diel vertical migration - an escape from invertebrate predators. Science 220, 1404–1407. https://doi.org/10.1126/science.220.4604.1404.

Østvedt, O.J., 1955. Zooplankton investigations from weather-ship M in the Norwegian Sea 1948-49. Hvalrad. Skr. 40, 1–93.

Parent, G.J., Plourde, S., Turgeon, J., 2011. Overlapping size ranges of Calanus spp. off the Canadian Arctic and Atlantic Coasts: impact on species' abundances. J. Plankton Res. 33, 1654–1665.

Peters, R., 1983. The Ecological Implications of Body Size (Cambridge Studies in Ecology). Cambridge University Press, Cambridge.

Planque, B., Batten, S.D., 2000. *Calanus finmarchicus* in the North Atlantic: the year of *Calanus* in the context of interdecadal change. ICES J. Mar. Sci. 57, 1528–1535. https://doi.org/10.1006/jmsc.2000.0970.

Planque, B., Hays, G.C., Ibanez, F., Gamble, J.C., 1997. Large scale spatial variations in the seasonal abundance of *Calanus finmarchicus*. Deep-Sea Res. Part I-Oceanogr. Res. Pap. 44, 315–326. https://doi.org/10.1016/s0967-0637(96)00100-8.

Plourde, S., Pepin, P., Head, E.J.H., 2009. Long-term seasonal and spatial patterns in mortality and survival of *Calanus finmarchicus* across the Atlantic zone monitoring programme region, northwest Atlantic. ICES J. Mar. Sci. 66, 1942–1958. https://doi.org/10.1093/icesjms/fsp167.

Reverdin, G., Niiler, P.P., Valdimarsson, H., 2003. North Atlantic ocean surface currents. J. Geophys. Res. Oceans 108. https://doi.org/10.1029/2001jc001020.

Richardson, A.J., Walne, A.W., John, A.W.G., Jonas, T.D., Lindley, J.A., Sims, D.W., Stevens, D., Witt, M., 2006. Using continuous plankton recorder data. Prog. Oceanogr. 68, 27–74.

Sætre, R., 2007. Driving forces. In: Sætre, R. (Ed.), The Norwegian Coastal Current - Oceanography and Climate. Tapir Academic Press, Trondheim, pp. 45–58.

Skarra, H., Kaartvedt, S., 2003. Vertical distribution and feeding of the carnivorous copepod *Paraeuchaeta norvegica*. Mar. Ecol. Prog. Ser. 249, 215–222. https://doi.org/10.3354/meps249215.

Skjoldal, H.R., Dalpadado, P., Dommasnes, A., 2004. Food webs and trophic interactions. In: Skjoldal, H.R. (Ed.), The Norwegian Sea Ecosystem. Tapir Academic Press, Trondheim, p. 493.

Skjoldal, H.R., Wiebe, P.H., Postel, L., Knutsen, T., Kaartvedt, S., Sameoto, D.D., 2013. Intercomparison of zooplankton (net) sampling systems: results from the ICES/GLOBEC sea-going workshop. Prog. Oceanogr. 108, 1–42. https://doi.org/10.1016/j.pocean.2012.10.006.

Speirs, D.C., Gurney, W.S.C., Holmes, S.J., Heath, M.R., Wood, S.N., Clarke, E.D., Harms, I.H., Hirche, H.J., McKenzie, E., 2004. Understanding demography in an advective environment: modelling *Calanus finmarchicus* in the Norwegian Sea. J. Anim. Ecol. 73, 897–910. https://doi.org/10.1111/j.0021-8790.2004.00857.x.

Staurland Aarbakke, O.N., Bucklin, A., Halsband, C., Norrbin, F., 2014. Comparative phylogeography and demographic history of five sibling species of *Pseudocalanus* (Copepoda: Calanoida) in the North Atlantic Ocean. J. Exp. Mar. Biol. Ecol. 461, 479–488. https://doi.org/10.1016/j.jembe.2014.10.006.

Strand, E., Bagøien, E., Klevjer, T.A., Broms, C., 2020. Spatial distributions and seasonality of four *Calanus* species in the Northeast Atlantic. Prog. Oceanogr. 185 https://doi.org/10.1016/j.pocean.2020.102344.

Sundby, S., 2000. Recruitment of Atlantic cod stocks in relation to temperature and advection of copepod populations. Sarsia 85, 277–298. https://doi.org/10.1080/00364827.2000.10414580.

Tande, K.S., Drobysheva, S., Nesterova, V., Nilssen, E.M., Edvardsen, A., Tereschenko, V., 2000. Patterns in the variations of copepod spring and summer abundance in the northeastern Norwegian Sea and the Barents Sea in cold and warm years during the 1980s and 1990s. ICES J. Mar. Sci. 57, 1581–1591. https://doi.org/10.1006/jmsc.2000.0982.

Torgersen, T., Huse, G., 2005. Variability in retention of *Calanus finmarchicus* in the Nordic seas. ICES J. Mar. Sci. 62, 1301–1309. https://doi.org/10.1016/j.icesjms.2005.05.016.

Wiborg, K.F., 1954. Investigations on zooplankton in coastal and offshore waters of western and northwestern Norway. Fiskeridirektoratets Skrifter Serie Havundersøkelser 11, 1–246.

Wiborg, K.F., 1955. Zooplankton in relation to hydrography in the Norwegian Sea. Fiskeridirektoratets Skrifter Serie Havundersøkelser 11, 1–66.

Wiebe, P.H., Morton, A.W., Bradley, A.M., Backus, R.H., Craddock, J.E., Barber, V., Cowles, T.J., Flierl, G.R., 1985. New developments in the MOCNESS, an apparatus for sampling zooplankton and micronekton. Mar. Biol. 87, 313–323.

Yen, J., 1985. Selective predation by the carnivorous marine copepod *Euchaeta elongata*: laboratory measurements of predation rates verified by field observations of temporal and spatial feeding patterns. Limnol. Oceanogr. 30, 577–597. https://doi.org/10.4319/lo.1985.30.3.0577.